DEDAN KIMATHI UNIVERSITY OF TECHNOLOGY

RANKING OF UNDEVELOPED KENYAN GEOTHERMAL PROSPECTS BY USE OF SURFACE GEOSCIENTIFIC DATA

By

RICHARD MUENDO KILEA

G082-01-0295/2018

GGL 4205: RESEARCH PROJECT

BSc Geology

Geothermal Training and Research Institute

Submitted on

28th November 2022

A RESEARCH PROJECT SUBMITTED IN PARTIAL FULFILLMENT OF THE REQUIREMENTS FOR THE AWARD OF DEGREE IN GEOLOGY, GEOTHERMAL TRAINING INSTITUTE (GeTRI), DEDAN KIMATHI UNIVERSITY OF TECHNOLOGY.

DECLARATION

I declare that this is my work and has not been submitted or approved in any university or college for the award of a degree.

Name: Richard Muendo Kilea

Signature:

Date:

Approval by supervisor

This project has been submitted for examination with my approval as the official University Supervisor

Name: Prof. Nicholas Mariita

Signature:

Date:

DEDICATIONS

I dedicate this research proposal to all the geothermal professionals and any other person who is interested in exploration and development of geothermal resources in Kenya.

ACKNOWLEDGEMENT

First of all, I would thank God for all he has done throughout my studies. Sincere gratitude goes to my Supervisor, Professor Nicholas Mariita, who has worked with me from the start of my project until the end of it. Without you, this project could not have been a success; I am grateful. Thank you sir!!

Lastly I would like to acknowledge Mr Cyrus Githua, from KenGen PLC for helping me obtain some of the data in needed in my project. Feel much appreciated for the contributions you have made.

ABSTRACT

Geothermal energy is thermal energy from the subsurface of the earth. The heat is extracted in form of steam, and is tapped in the surface at very high pressures. Geothermal energy is renewable, carbon free and free form of energy that provides a continuous and uninterrupted supply of power and heat. Utilization of Geothermal energy began in the early 19th century and as civilization advanced, this form of energy became most preferred and thus there is need to increase its capacity because it is not fully utilized. Kenya is endowed with this form of energy along the rift valley due to the recent quaternary volcanoes. Currently Kenya has an installed capacity of over 900 MWe, however the geothermal capacity in the country is more than 7,000 MWe. Only 5 of the 14 geothermal prospects have been developed while the rest are in different stages of exploration. This project highlights the geothermal portfolio capacity in Kenya and ranks the remaining 9 geothermal fields in their order of development. These fields include; Emuruangogolak, Suswa, Longonot, Arus Bogoria, Lake Baringo, Silali, Namarunu and Barrier geothermal field. To achieve this ranking, surface geoscientific data was generously given by various sources such as the main two industrial geothermal players (KenGen and GDC) and the Ministry of Energy. The data was reviewed and integrated to come up with a basis for the classification and ranking. Using this data, the project developed detailed raw conceptual models of each geothermal field and power potential estimates using power density calculations. Power density method of geothermal power calculation gives first order estimates of the geothermal filed expressed in terms of MW/km^2. Results of this work has ranked the fields as follows: Taking the resource capacity estimates, geological, hydrogeological, and fluid chemistry criteria into consideration and some socio-economic factors, the geothermal prospects are ranked as follows: Suswa, Longonot, Silali,

Emuruangogolak, Korosi, Barrier, Arus Bogoria, Lake Baringo and Namarunu; Suswa being the most viable.

CONTENTS

LIST OF FIGURES

LIST OF TABLES

1 INTRODUCTION

1.1 BACKGROUND INFORMATION

For a Perfect Geothermal system to exist, certain conditions must be present. These 3 conditions include: heat source, which is the critical factor, reservoir with a recharge system and structures such as faults or fracture or permeable formation as shown in Figure 1.1. Ideal areas with these set of conditions exist in active plate boundaries or in young volcanic centers. The Kenya Rift Valley which is a part of the East African Rift System (Calais et al., 2006) is endowed with such ideal conditions. The Kenyan rift valley is lies in active plate boundaries (Nubian and Somali). This tectonic setting has fundamental influence and controls the stress regime, thermal regime, hydrogeological regime, fluid chemistry, fluid dynamics, faults and fractures, and lithological sequence (Rybach, 1981). Our geothermal potential is up to 10000 MWe (Omenda, 2015) in all the prospect areas along the rift valley. These prospects lie along the rift's axis extending from lake Magadi in the south to Barrier volcanic complex in the North. However, we have an installed capacity of less than 1000 MWe. The Kenyan government came up with a 2030 vision plan to increase the installed capacity to 5560 MWe. To achieve this, we must have a development plan. A proposed geothermal field development is subdivided into 3 principles: Portfolio exploration, Stepwise expansion and Parallel development(Mangi, 2018). This research project fulfils the Portfolio principle by exploring fields and evaluating them simultaneously thereby increasing the probability of having at least one viable prospect for development at any given time while reducing the chances of overlooking significant development opportunities. Exploration in Kenya began in 1960 with two exploration wells in Olkaria. The step wise expansion involves cautious incremental step development determined by reservoir data. This reduces the risk of reservoir depletion and

pressure drops. This is achieved in the research project by coming up conceptual models. Conceptual models help in monitoring geothermal reservoir changes during long times exploitations(Axelsson et al., 2013). Parallel development principle involves development of fields selected from portfolio exploration and developing them. This is principle can be achieved by public and private investments. These principles speed up the development plan for 2030. Currently some of the resources are well developed and in exploitation and utilization, whereas some are in various stages of exploration. Key prospect areas in Kenya include: Barrier, Badlands, Emuruangongolak, Korosi, Paka, Arus, Suswa, Akiira one, Eburru, Namarunu, Longonot, Silali,

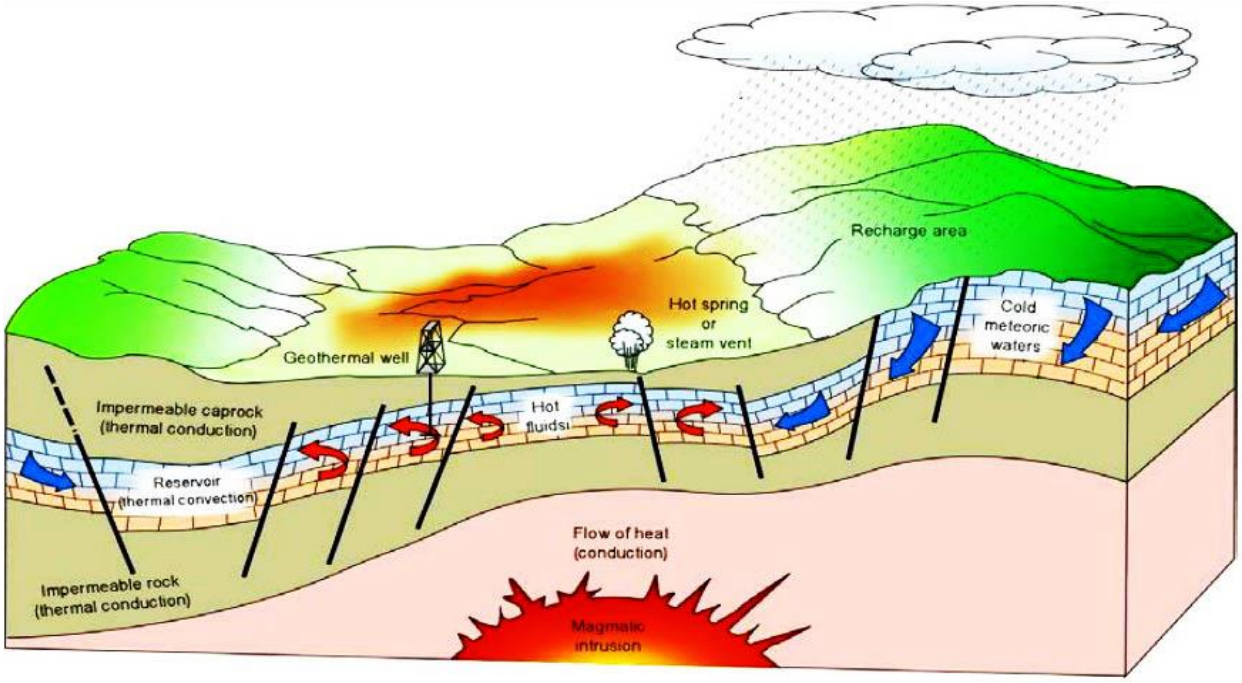

Figure 1.1: A complete geothermal system (Gehringer and Loksha, 2012)

1.2 SCOPE OF THE RESEARCH

The study is restricted only in the Kenyan Rift valley. This study is based on data from various company reports which have been licensed to explore geothermal energy in Kenya.

The study is thus limited to geothermal exploration. Geological, geophysical, geochemical and GIS data will be used to explore and evaluate geothermal prospects along the Kenyan Rift valley. These data will help in focusing on resource characteristics and come up with conceptual models for resource development.

The main objective of this study is to integrate Geo- Scientific data to evaluate and map all geothermal prospects in Kenya and categorize them in their rank of development. Project prioritization and ranking is usually perceived as an initial step, a decision point that leads to the actual execution of the project.

1.3 STUDY AREA

The study area is approximately 1000 km and runs from the Barrier to Lake Magadi as shown in Figure 1.2. Kenyan rift valley is next area of interest for development as a source of electricity in Kenya with ownerships of the resource in the field belonging to different companies such as Kengen, GDC and other independent power producers. Some of these prospects have been developed and in utilization while others are still under exploration

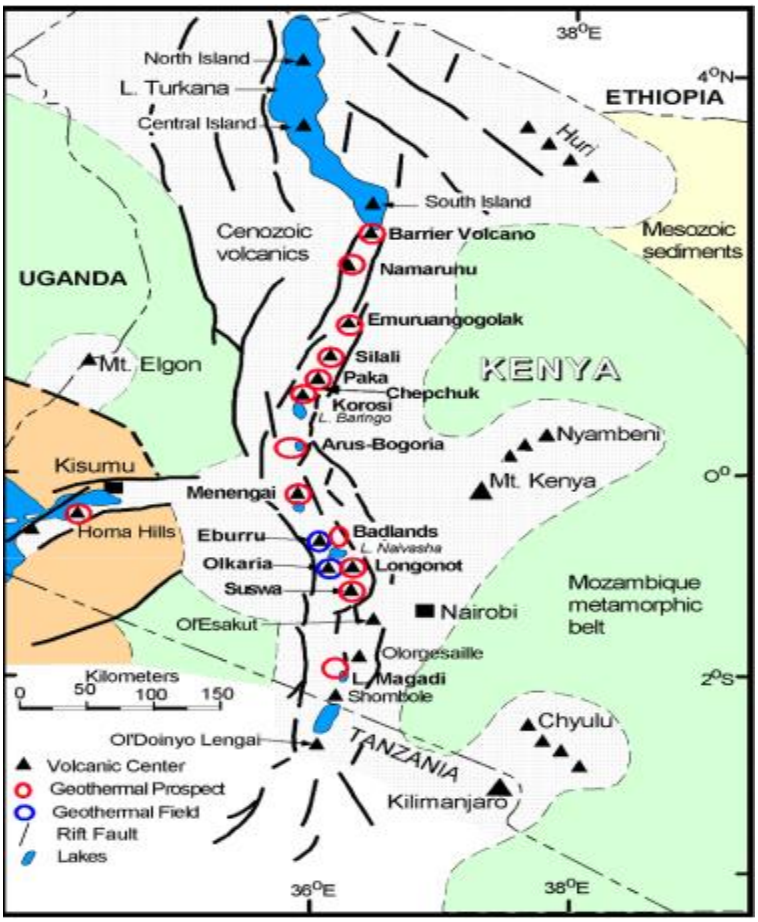

Figure 1.2: Simplified geological map showing geothermal prospects (Omenda and Simiyu, 2015)

1.4 PROBLEM STATEMENT

Data has been collected over the years by various researchers assessing the potential of geothermal of each prospect. Most of the prospects have surface exploration data. Only Olkaria, Eburru, Menengai, Paka and Korosi have information from drilling which can be used to approximate the geothermal potential of each of the drilled fields. However, Emuruangogolak, Suswa, Longonot, Arus Bogoria, Lake Baringo, Silali, Namarunu and Barrier Geothermal fields have not been drilled and these prospects are the main focus of this research project. There is need to rank these field with surface data so as to prioritize the sequence of exploration drilling.

1.5 OBJECTIVES OF THE STUDY

To rank the undrilled geothermal prospects in Kenya with maximum chances of success in the future the research aims to address the following objectives:

I. Reviews all the known surface geoscientific data of each prospect and come up with a raw conceptual model. This model will give more insights about the geothermal system.

II. Determine the areal extent of each field. The potential will be determined using resistivity anomaly maps.

III. Determine resource capacity estimates using power density method.

1.6 JUSTIFICATION

Ranking of the undrilled geothermal fields is important because it helps focus on which field to prioritize when it comes to development. We have several options here but we have to focus on the resource characteristics and the output of the field and power potential compared to other fields. What will be the power potential of one field compared to other fields according to the available data, what is the condition of the established infrastructure, what is the availability of resource appropriate distance and what are the exploration challenges. These are some of the questions that contribute to this ranking of the field.

1.7 OUTPUT AND EXPECTED RESULTS

The research has provided a clear classification of the geothermal fields according to their priority of development.

2 LITERATURE REVIEW

2.1 HISTORIC BACKGROUND

Geothermal energy doesn't have much cache as other energy and it's been there since our entire arc of civilization. Hot pools and hot springs have been used for bathing, heat treatments, heating and cooking. These are classical examples of direct use of the geothermal resources. The resource was also be used for producing salts from the hot brines. Natural geothermal springs have also been used in some parts of the world as symbols of life and power (civilization and religion) it was until the 19^{th} century when thermodynamics was discovered. Thermodynamics helped revolutionize geothermal energy by efficiently converting energy from hot steam to mechanical energy and then into electrical energy (Kanoglu, 2002). This was aided by use of turbines. This technology was associated with Larderello region of Tuscany in northern Italy (Parri et al., 2016). The first power plant went into operation in the year 1913 producing an electrical power of 250 Mwe.

In Kenya geothermal exploration began as early as 1950s when two exploration wells, we drilled in Olkaria supported by the United Nations Development Programme. Furthermore, a British-Kenya geothermal exploration project was undertaken between 1985-1987, as part of a regional resource assessment (Allen et al, 1989). Further investigation has been done on the Kenya rift valley and development made on various fields such as Olkaria, Menengai and Eburru. Currently Kenya has an installed capacity of 799 MWe.

2.2 GEOGRAPHIC LOCATION AND GEOTHERMAL RESOURCES

Geothermal energy resources are concentrated to a large extent along certain well-defined belts. These belts of high volcanic activity are associated with earthquake activity and recent volcanism. These belts of high volcanic activity, seismicity and hot spring activity are associated with geological boundaries and cover approximately 10% of the earth surfaces. The world's most outstanding geothermal belt is the circum-pacific belt as shown in Figure 2.1. One branch extends through central America to the western portion of south America and then Antarctica. Another branch of the belt runs through the East Pacific Region through New Zealand, New Guinea and Indonesia. And then branches out north, running through Philippines, Japan and Eastern Siberia, it then turns eastwards through Aleutians back to the New Canada. Another outstanding geothermal belt runs through East Africa, Ethiopia, Kenya and Tanzania and gradually weakens southwards. The mid – Atlantic Ridge belt usually runs underwater. However, where islands have formed following volcanic eruptions associated with separations of the major earth plates, considerable geothermal activity is to be found, as in Iceland or in the Azores chain. Geopressured resources are also abundant in many major sedimentary regions of the world, including the Gulf coast of the United States, western Indian and Persian Gulf (Tester et al., 2007).

Temperature of the earth's crust increases with depth at varying rates, depending on location. The normal temperature gradient is about 25°C /km depth. Thus, in an ambient surface temperature (mean annual temperature) is 15°C, it is expected that at random hole drilled to a depth of 1 km will encounter a temperature of 40°C (the ambient temperature plus the temperature increase due to normal temperature gradient in the region) however in some regions of the world, the temperature gradient is much greater than normal, increasing in places to a gradient as high as 1°C

/M. In those areas associated with recent volcanism, relatively high temperatures may be encountered at shallow depth.

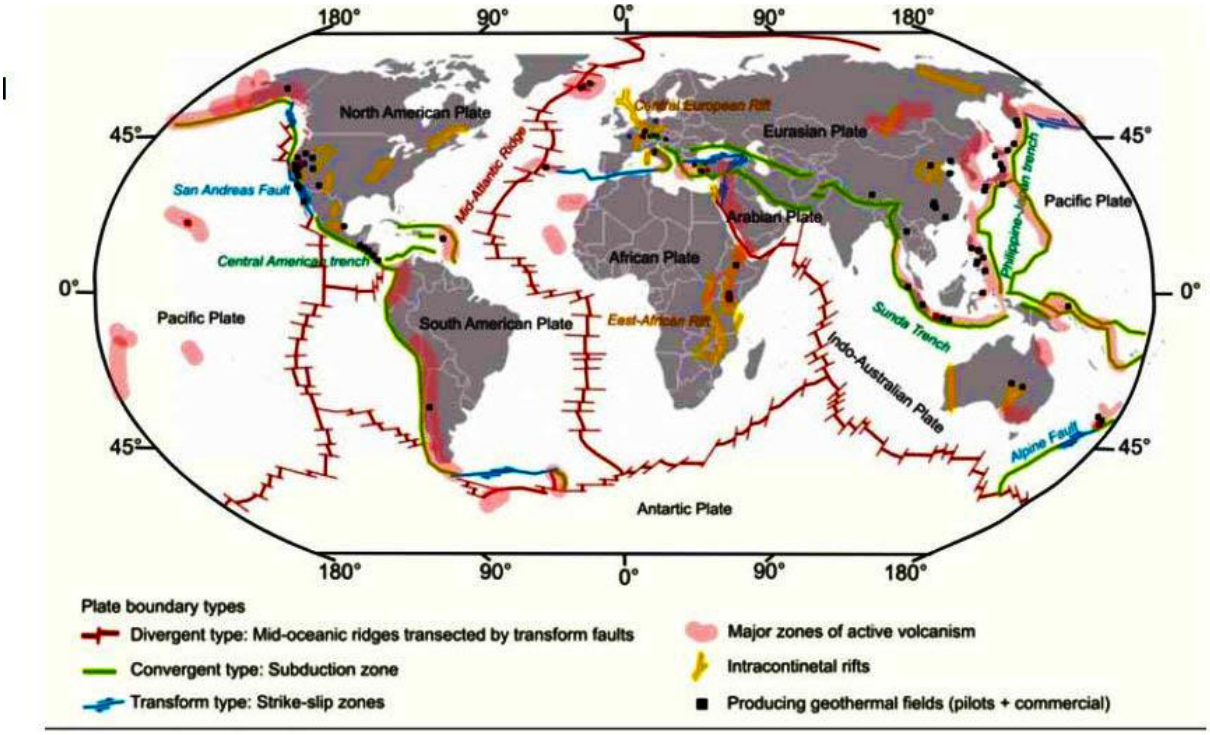

Figure 2.1: Plate tectonic setting of installed geothermal systems worldwide (Gehringer and Loksha, 2012).

2.3 TYPES OF GEOTHERMAL SYSTEMS

There are 4 types of geothermal systems, Liquid Dominated and vapor- dominated hydrothermal systems, Hot dry rock systems and Geopressured systems (Saemundsson et al., 2009). These types are characterized by their difference in their thermodynamic and hydrologic properties as discussed in the following sections.

2.3.1 Liquid-dominated Systems

Liquid dominated geothermal resources are those that are controlled by the Prescence of circulating liquids (water or brine) that can transport the thermal energy of the rock from deep regions to near surface regions by natural circulations. The temperature of liquid dominated geothermal systems varies from being ambient or slightly above too high as 360°c. Most investigations indicate that liquid dominated resources are far more abundant than the vapor dominated. Usually, the temperature in the best liquid geothermal regions increases rapid with depth until the temperature reaches the boiling point of water. Further increase in temperature with depth will be slight until a depth is reached where liquid domination ceases. Temperatures seldom exceed the boiling point of water at prevailing hydrostatic pressures.

2.3.2 Vapor dominated systems

Vapor dominated systems, sometimes referred to as dry steam fields and are relatively scarce. However, the most impressive and successful geothermal power development in the world is associated with the development of vapor dominated systems e.g., Lardello, Italy, The Geysers, California and Japan. In such systems the continuous phase within the pore spaces near surface region is that of steam, while in deeper regions water is presumed to be present. Temperatures are typically in the range of 220-150°c. Production of steam from this type of reservoir is relatively simple and quite often a slight superheating of the steam occurs during production.

2.3.3 Hot dry rock systems

Geothermal gradient increases with depth independent of the hydrothermal convection, however porosity decreases with depth due to pressure. So, it is reasonable to say more heat is stored in rock matrix as compared to circulating waters and this proves vast volumes of hot dry rock exist

at depth. More research is undergoing to develop methods of introducing cold waters into the hot dry rocks with artificially induced fractures and extracting this heat through a pattern of drilled well (Brown et al.,2012). Calculations suggest that heat reserves in a known geothermal system is much larger than the heat contained in the circulating fluids. It is possible that today's hydrothermal systems such as Olkaria may be further exploited as hot dry rock systems at sometimes in the future.

2.3.4 Geo- Pressured systems

Geopressured reservoirs are generally located in deep sedimentary strata in geologic regions where sediment compactation has taken place over long geologic periods and where an effective shale cap has formed (Debout et al., 1982). Under conditions of shale compression, in which water is squeezed out of the shale matrix into adjacent sand bodies, an internal pressure greater than the ordinary hydrostatic pressure at that depth is imparted to the water. In extreme cases of geopressure, water pressures approach those of the overall weight of the overlying rocks (close to lithostatic pressure). This over pressured water system, known as a geopressured geothermal resource is often characterized by higher-than-normal temperature gradients because of the increased specific heat capacity of the over pressured rock-water systems. Temperatures as high as 237°c have been encountered in some geopressured zones in the Gulf Coast of the United States, with well head pressures in excess of 7.6×10^7 Pa (11,000 Psi) (House et al.,1975). In addition, geopressured fluid typically contain enormously high concentrations of dissolved methane gas. Practically all large synclinal basins of the world contain some geopressured zones. This geopressured systems are mostly developed in the USA.

2.4 REGIONAL GEOLOGY

The East African Rift System serves as a classical example of continental rift which is in its initial stage of continental break up (Achauer and Masson, 2002) with underlying mantle plumes. Its evolution is considered to be structurally controlled (Smith and Mosley, 1993) this is explained by studying contact zones i.e., the Proterozoic Orogenic belts and the Achaean Tanzanian Craton by Rift faults (Shackleton, 1996). When we look at the Turkan south we see the Rift is divided into two distinct branches that encircle Tanzanian Craton, an older volcanic active western (Ring, 2014). The eastern branch extends from the Red sea in Afar region and passes through the main Ethiopian Rift, the Kenyan Rift valley and the Tanzanian Basin divergence before terminating further in Mozambique (4000 Km) the young western branch extends a distance of 2000 km from lake albert to lake Malawi (Chorowicz, 2005)

The EARS resembles a trough which is 40 to 65 km wide and transverses two broad, elongated domal uplifts i.e., Kenya and Ethiopia. The elevation of the rift floor is highest in the central part of the domes in Kenya (2000m), followed by Ethiopia which is 1700m and decreases progressively to the fringes. The Afar Triangle (shown in Figure 2.2) which is a triple junction between the African, Arabian and Somalian plates (Chorowicz, 2005), is an important structure in the entire rift interplay as it connects the EARS to two oceanic rift systems; the Red Sea and Gulf of Aden.

The evolution of EARS dates back 25-30 million years ago (Ring, 2014). Rifting continued developing as a result of voluminous mantle plumes. This is called the African super swell which continued impinging upon the base of a stretched continental lithosphere (Ebinger and Sleep, 1998). The driving energy of this process is the hot atmospheric plume emanating from the top the African super swell in the upper few hundred kilometer of the mantle (Ebinger and Sleep, 1998).

To date still exists some plumes influencing both tectonics and magmatism beneath the EARS. However, questions and debates still exist about the depth of the Hot material and their continuity.

Based on observations and plate analysis, the EARS spreads at different rates with the most active spreading center at the Red sea – Gulf of Aden area, approximated at ~2 cm/year. In the Main Ethiopian rift, it is estimated at ~1 mm/year, and further less than 1 mm/year in the Kenyan Rift and southwards (Ring, 2014)

Propagation of the rift began as a chain of marginally warped depressions, which were accentuated as domal uplift proceeded, until, in mid-Miocene to early Pliocene times, faulting produced asymmetrical grabens. The final uplift phase in the early Pleistocene was accompanied by major graben faulting, and subsequent faulting has intensely fractured the floor of the rift along an axial zone marked by caldera volcanoes. Seismic velocity information from refraction measurements and tomography experiments, reinforced by gravity studies (Ebinger, 2005), indicate that the eastern rift lies along a zone of progressive crustal thinning with local crustal disruption.

According to Baker et al. (1972) the uplift of the Ethiopian and Kenyan domes has been synchronous in three major pulses of late Eocene (44-38 Ma), MidMiocene (16-11 Ma), and Plio-Pleistocene (5-0 Ma) age. Volcanism of intermediate and salic type displays some relation to uplift in time and space and to the onset of graben faulting. However, major flood basalt extrusions in the early Tertiary in Ethiopia were related to massive crustal warping along the future rift margins (Williams, 1970). The volcanism associated with EARS is overwhelmingly alkaline, and at some volcanoes a strongly alkaline fractionation series is distinguishable from a more mildly alkaline series (Williams, 1970). The flood phonolites, trachytes, rhyolites, and ignimbrites of Kenya, and the pantelleritic ignimbrites of Ethiopia, could have resulted from anatexis of a mantle-derived accreted layer at the base of the crust (Baker and Wohlenberg, 1971).

The evolution of the KRS, a complex graben ~ 40-65 km wide bounded by major rift faults arranged *en echelon,* dates back to the East African orogeny. The rift bisects the Kenya domal uplift, which itself is superimposed on the eastern margin of the East African plateau (Baker et al., 1972). The KRS is also located close to the boundary of the Tanzanian Craton and the Pan-African Mozambique shear belt. Volcanism associated with the KRS started during the Miocene epoch (~ 24 Ma), resulting in widespread basaltic eruptions in the Turkana topographic depression, a failed Mesozoic rift system (Boone et al., 2019). The Miocene basalts were subsequently faulted and followed by the relatively extensive, reliably dated flood phonolites. The latter are of chemically homogeneous composition and were erupted from the crest of the Kenya dome in the late Miocene and early Pliocene (Baker et al., 1972). The total volume of eruptive rocks is estimated to be > 220,000 km3, with a thickness of up to 900 m, as revealed by faulting at the rift margins. In an important contribution, Ebinger and Sleep (1998) suggest the flood phonolites to be a product of partial melting of the lowermost part of the crust.

Volcanism off the rift axis was concurrent with the rifting process and is responsible for the formation of the vast, uplifted, off-rift volcanic centres, namely Mt. Kenya, Chyulu and Huri hills, located on the eastern flanks. It has been observed that these three sites of domal uplift are not rifted, and, support a model whereby doming predated rifting (Wilson, 1989). Further block-faulting of the Miocene volcanics produced noticeably massive and extensive, more evolved eruptions of trachytic ignimbrites in the central area, provisionally assigned to lower Pliocene (Ring, 2014). The trachytic ignimbrites formed the Mau and Kinangop tuffs. A third faulting episode, which followed the ignimbrite eruptions, resulted in the formation of the graben structure, as it is known today (Baker et al., 1972). In the developing graben, successive fissure eruptions produced approximately 900 m thick layers of trachytes, basalts, basaltic trachyandesites and

trachyandesites. The plateau rocks that filled the developing graben were subsequently block-faulted to create high-angle normal faults, which are common in the axial graben of the rift floor. The fractures apparently served as conduits for a series of Quaternary volcanoes of basaltic to silicic composition (Ebinger and Sleep, 1998).

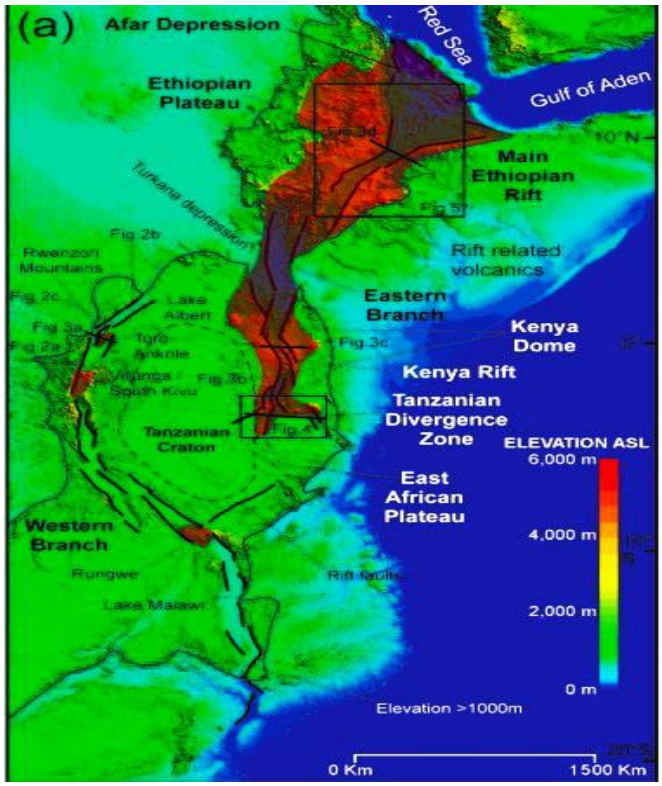

Figure 2.2: The EARS showing the eastern and western branch ((Chorowicz, 2005)).

.

This Gis model is developed from data that is openly available online, hosted by BGS national Geoscience Data center.

(https://www.bgs.ac.uk/services/ngdc/accessions/index.html#item132705)

2.5 LOCAL GEOLOGY

The Kenyan rift valley is marked by anomalous hot mantle upwellings throught its history in the Miocene period to present day. This volcanic activity is confined in the Rift zones and extends east and west but is more broadly centered on the Kenyan domes. The Kenyan domes show a diversity in composition ranging from acidic-basic, but mostly are characteristically alkaline varying (mildly alkaline, alkali basalt trachyte series to strongly alkaline) and undersaturated nephelinites and phonolites (King, 1978). The magmatic activity in the rift was accompanied by domal uplift of about 300m on the crust of which erupted phonolites (Hay and Wendlandt, 1995). The rifting also provided the throughs that formed the lakes that are alkaline and the geology is composed of Precambrian basement, tertiary rift volcanics and sedimentary deposits to the north.

2.6 STRUCTURAL GEOLOGY

The EARS is a system of normal faults bordering a 40-60 km wide trough, funneling out toward north in the Afar region (Figure 2.3). The Kenya Rift diverges into splays towards north (Turkana) and south Tanzania (Baker et al, 1971). Domal uplift and extension causes the brittle crust to fracture into a series of normal faults giving the classic horst and graben structure of rift valleys.

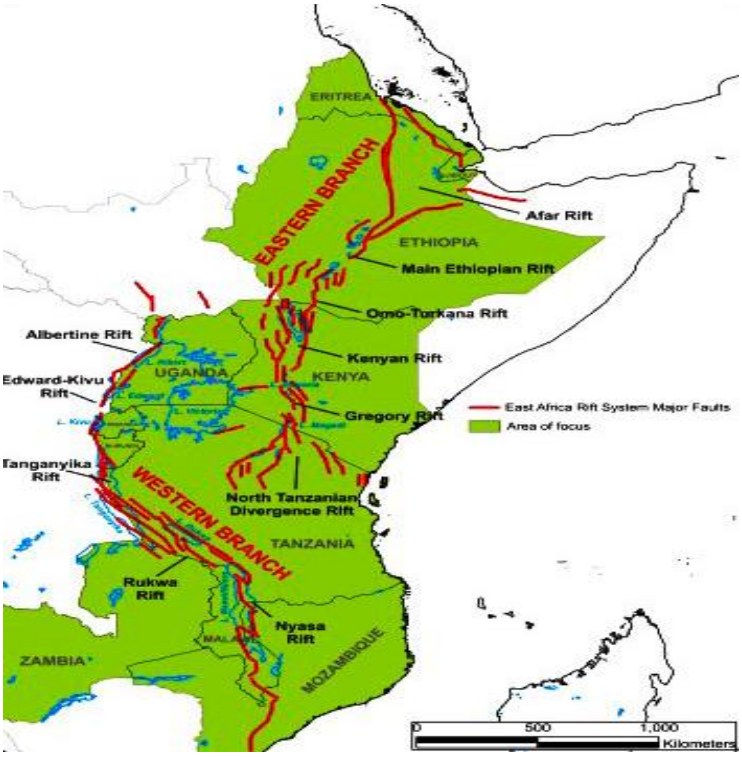

Figure 2.3: A map illustrating the East African Rift System with the red lines indicating the major faults lines. The fault interpretation has been adapted from (Chorowicz, 2005).

2.7 GEOTHERMAL MANIFESTATIONS

Geothermal manifestations in the Kenya rift include fumaroles, hot springs, spouting springs, hot and altered grounds and solfatara (Sulphur deposits). Fumaroles commonly occur on the mountains while hot springs and geysers are common on the lowlands. Sulphur deposits have been observed at several geothermal areas including Olkaria, Paka and Barrier volcanoes where it is indicative of the Presence of a degassing magma body at depth (Simiyu, 2010). Extinct manifestations in the form of travertine deposits, silica veins and chloritized zones are common in the Lakes Baringo – Bogoria regions indicating long-lived geothermal activity in the rift.

2.8 GEOTHERMAL START UP AND PRE-FEASIBILITY STUDIES

After the preliminary survey which involves hydrogeological, geological, surface manifestation and anecdotal information, the next step involves exploration phase. The purpose of exploration is to delineate resource temperature, depth and productivity prior to field development. The exploration phase starts off at a more regional level and further narrowed down to more localized regions. Exploration initially begins data collection from appraisal wells or neighboring wells as well as other surface manifestation and further more goes down to subsurface surveying using Geochemical, geological and geophysical methods. It may to some extend involve environmental studies. Some of these techniques are used in the study are:

2.8.1 SURFACE STUDIES

This is the initial step in field exploration and it is purposed for location and characterization of all the geothermal features in different prospects. This surface studies should include stud of geothermal manifestations such as solfataras, fumaroles, hot springs, gas seeps and mineral springs. Location and names of the geothermal features, as well mapped extent of surrounding geothermal deposits is compiled on a single map for each prospect with consistent geological and tectonic settings. All of these data should be georeferenced, allowing for easy integration with other project data. A thorough analysis of the active geothermal features would give an estimate of the rate of geothermal fluid movements within the system and a rough idea of the extent and geometry of the geothermal resource. The following are expected at the end of the surface studies; Location, Presence of odors (sulfur or other odors), Presence of gas bubbles and their compositions and a detailed local map of areas with thermal features clearly labeled.

2.8.2 GEOLOGICAL DATA COLLECTION

A good understanding of the geology of the project area and how it fits into the surrounding geological and tectonic environment is important in understanding a given geothermal system. Geological studies initially should be focused on understanding the overall geology and identifying the most promising areas. These studies should establish permeability pathways that bring thermal fluids from deeper parts to the shallower parts of the system. This geological data should be presented in form of geological maps, stratigraphic columns, structural maps and cross sections. Overally the data collected should address stratigraphy, lithology, geological structure, tectonics, hydrothermal mineralization and sense of movements. After the field development, 3-D geological models can be developed using specialized modelling and visualization software. The geological history of the area should be summarized in a different document, including a description of the local stratigraphy, the lithological units expected during drilling, and a summary of the types, locations, and nature of geological structures.

After a good analysis of the Geology, one should come up with a clear representation of the regional and the local geology, stratigraphy and tectonic structure of the area as well as identification of uncertainties and data gaps that need to be addressed in successive stages of exploration. This data should indicate which structures and which units could host a geothermal reservoir, and forms the basis of subsequent conceptual and numerical models.

2.8.3 GEOCHEMICAL DATA COLLECTION

Geochemistry plays a key role in exploration for high enthalpy geothermal resources. Sampling, analysis and calculation of Geothermometry provides estimates of the potential resource. Interpretation of geochemical data can be very useful during the Exploration Phase to develop an understanding of the temperatures and extent of the geothermal reservoir and to ascertain whether

the resource is sufficiently well developed and hot enough to be utilized for geothermal electrical generation. Geochemical studies should be focused on understanding parameters such as estimated resource temperature, the origin of the fluid, location of different aquifers, mixing of aquifer fluids, source and recharge of the geothermal of the geothermal system, pathways for discharge from the geothermal system and the potential for corrosion of the geothermal fluids. Fluid and gas geochemical data are represented on maps, tables, drawings, and plots of the project area. Some of the surveys conducted include;

2.8.3.1 SOIL SAMPLING

Sampling of (CO2) soil flux in soil is another commonly used geochemical tool in geothermal systems, this is because geothermal systems contain non-condensable gases. Therefore, soil sampling surveys are designed to locate anomalously high concentrations of CO2 that indicate a potential geothermal system at depth. Increased CO2 flux occurs near many active geothermal manifestations, and CO2 flux can suggest a geothermal system at depth. CO2 soil flux surveys are done with a portable meter that measures the active flux of CO2 through the soil. While CO2 soil flux surveys can show the presence of active geothermal manifestations and structures such as faults that may be conducting geothermally-derived gases toward the surface, these surveys rarely provide significant geologic or geochemical insight. However, they can often confirm the results of other methods (notably geologic mapping), and they are reasonably cost-effective

2.8.3.2 FLUID AND GAS SAMPLING

After identifying and characterizing geothermal manifestations such as fumaroles, geochemical samples are collected of the representative steam, fluids, and gases. If the geothermal manifestations are numerous, it is recommended that you prioritize those with high electrical conductivities and those with high temperatures, or if there are multiple with comparable

temperatures and electrical conductivities, you prioritize the ones with high heat flow rates. Suppose from the analysis the temperatures and conductivities show the hotter and colder waters mix. In that case, a range of samples should be collected to understand how the thermal fluids mix and with other compounds.

In a case where geothermal manifestations are not located, springs with high electrical conductivity, gas bubbles, and unusual gas odors are sampled. These attributes result from input of thermal fluids in most cases. The following characteristics are recorded in fluid and gas sampling; location (UTM), temperature in degrees Celsius, Electrical conductivity, flow rate in liters per second, PH, Prescence of odors, presence of gas bubbles, and Presence of precipitate. The samples fluids should be taken to the lab to further analyze cations, anions, silica, and isotopes in water and sulfate. The completed analysis is compiled in a database or a spreadsheet. It is important to note that Geothermometers respond to cooling at different rates and are affected differently by various rock types and other reservoir conditions; therefore, it is necessary to calculate the geothermometers as a suite, within their geologic context, in order to properly estimate potential resource temperatures. Chemical parameters should be plotted against each other in a variety of plots to assess the characteristics of the geothermal fluids.

Good results of geochemistry studies should indicate the temperature distribution within the geothermal system, the maximum temperature range for the resource, and the fluid-mixing model and, as with geologic studies, the identification of uncertainties and data gaps that need to be addressed in the following stages of exploration.

2.8.4 GEOPHYSICAL DATA COLLECTION

Another indispensable tool in geothermal exploration is geophysics. This tool helps us understand about the stratigraphy, structure and heat flow. Input from experienced geothermal scientist helps in identifying which geophysical techniques is the most appropriate and which technique is most cost effective. There is different type of Geophysical surveys which include; gravity surveys, electrical and electromagnetic resistivity surveys (specifically magneto-telluric (MT), seismic surveys (both 2D and 3D surveys) and temperature gradient drilling (also known as heat flow surveys). In some geological settings such as Geo-pressured systems which have sedimentary rocks seismic reflection surveys provide valuable information about the depth to lithologic units (stratigraphy), reservoir rocks and the faults that offset them, but the value of the additional data might not always justify the cost of running the survey, therefore geophysical surveys should be soundly planned before being carried out.

Geophysical data collection points should be presented on maps with license boundaries and cross section lines clearly labeled. Maps should be provided as geo-referenced digital files or have a grid overlain on them that allows for easy geo-referencing (including UTM coordinates or latitude-longitude, with appropriate projection and datum information). In addition, cross section views should be provided as appropriate for the data sets, including orientations that are parallel and perpendicular to the regional geological structural trends. Below are some of the techniques used in the study:

2.8.4.1 GRAVITY SURVEYS

Gravity surveys measures the bulk density of rocks beneath the prospect/project area. This technique helps asses the stratigraphy and structure of the subsurface by measuring thickness and density of different sub surfaces. Data from gravity surveys is usually integrated with geological

maps to have better insights into the 3-D distribution of rocks as well as the geological structure of the area. Gravity surveys apply bot regionally and locally during exploration phase and its one of the easiest of all geophysical technique. It is also cost effective and is a fundamental technique used in exploration of many types of natural resources including geothermal. Sometimes magnetic data can be incorporated to add information about the stratigraphy and structure. Gravity data is presented in form of contour maps of complete Bouguer and residual gravity, with the appropriate reduction densities indicated. Two- or three-dimensional models fitting the data should be provided in the form of maps and cross sections that show the measured and collected results.

2.8.4.2 ELECTRICAL RESISTIVITY SURVEYS

Electrical resistivity tools are a quite valuable tools in geothermal tools but has some limitations. There are various resistivity methods including; DC resistivity surveys, vertical electric soundings (VES or ―Schlumberger soundings), magneto-telluric (MT) surveys, time-domain electric magnetic (TDEM) surveys, and controlled-source audio-magneto telluric (CSAMT) surveys. Currently the most common resistivity technique is geothermal exploration is magneto-telluric (MT) because it can measure rock resistivity (or conductivity) to deep levels (a few km, which is significantly greater than for most other methods).

First application of resistivity surveys was in volcanology to explore high enthalpy geothermal resources>200°C in high enthalpy fields a cap of hydrothermally altered clay exists above the reservoir. Resistivity surveys can be used to image the clay alteration because they are zones of low resistivity while the reservoir is a zone of high resistivity. Resistivity surveys can be performed on both regional and local scale and it is usually important to conduct other geophysical surveys and then supplement with a more detailed resistivity survey, with perhaps as many as 10-15 stations per square kilometer.

Resistivity data when incorporated when incorporated with other data such as temperature gradient data can be helpful in identifying locations of deep, full diameter wells. Resistivity data is presented in a similar way as gravity data in form of contour maps of conductivity/resistivity at a particular depth/elevation or iso-resistivity contour maps showing the elevation of a particular conductivity/resistivity value. Cross sections showing resistivity distribution are ideally presented along the same profiles as presented in gravity data.

2.8.4.3 TEMPRATURE GRADIENT DRILLING

Temperature gradient is another indispensable geophysical tool although it is regarded as more of a drilling method. This method targets to determine resource temperature or quantity of Heat. Temperature gradient wells are often drilled with water-well rigs, which makes gradient drilling a cost-effective tool. The main objective of such drilling is to obtain temperature gradient information which will improve the confidence around temperature and depth predictions. Slim-hole drilling may be especially useful to resolve ambiguities in the interpretations of geoscientific surveys, especially in areas where temperature data are missing due to the absence of sufficient exploration wells. This method is used towards the end of exploration phase, focusing more on areas deemed to be most promising based on earlier exploration and analysis. This enables an evaluation of the variation in temperature gradient across an area. Temperature Gradient is an excellent complement to chemical Geothermometry, which estimates the temperature at the fluid source, but its unable to say what depth that fluid might be found (delineate conductive zones from zones of convection; identify zones that are transferring heat through convection; quantify the conductive flux of thermal energy through the area; and allow more accurate extrapolation of temperature to greater depth so long as the bottom of the hole is in a conductive zone). Occasionally Temperature Gradient might encounter a shallow geothermal resource. In such

instances, this becomes an opportunity to collect additional information that are useful in understanding the system e.g., if it is possible to collect fluid samples by briefly flowing of bailing the well.

If the drilling permit does allow such activities, it may be possible to conduct a short injection test of the well. Injection test data, together with stabilized temperature profiles can be used to estimate the productivity of a full diameter well drilled into similar condition. Temperature data can be presented on maps at specific depths or elevations by contouring temperatures, temperature gradients, or heat flow values, and on cross sections that include the shallow geology and may show how temperature gradient and heat flow changes with depth (owing to the variation in the thermal conductivities or movement of heat through convection)

2.8.4.4 SEISMIC SURVEYS

This is the most common geophysical tool in oil and gas exploration. This technology can be borrowed however the value of the of the resource to the cost of the method should be considered (oil and gas have far more value per unit measure compared to geothermal). A second reason is that geothermal is hosted in volcanic rocks as compared to oil and Gas which are hosted in sedimentary rocks. However, in geopressured systems come very often along sedimentary layers of karst formations. In this low- medium enthalpy systems 2-D seismic reflection can be used to identify faults and other extensive structures. High enthalpy geothermal systems tend to be hosted in deformed metamorphic and volcanic rocks that are characterized by less lateral continuity, which results in seismic data sets that are difficult to interpret, therefore the application of reflection seismic methods in geothermal exploration and development tends to be limited to areas where both geologic and economic conditions support its use

Good outcomes of geophysical investigations include, but are not limited to; an indication of the temperature distribution both horizontally and vertically, improved knowledge of the geological structure and stratigraphy, and indications of fluid migration pathways and reservoir boundaries. Figure 2.4 represents a seismic micro section drafted from geothermal handbook.

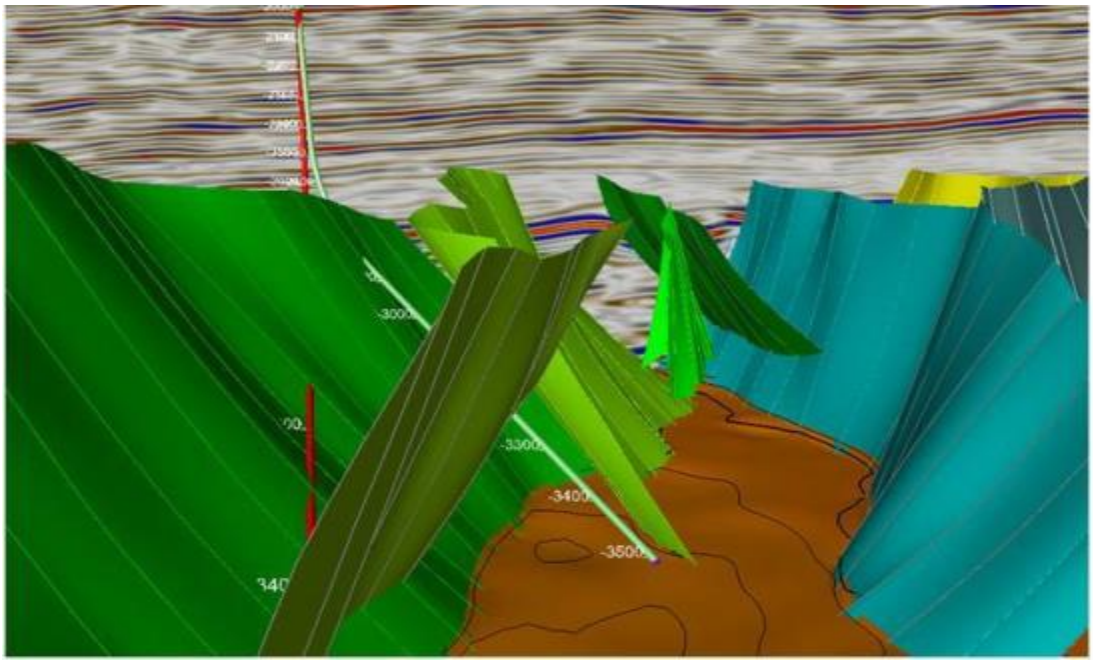

Figure 2.4: Example of seismic section with geological interpretation (Bauer et al, 2014)

2.9 CONCEPTUAL MODEL

By the end of the exploration phase, a conceptual model is developed to organizing and integrating geoscientific data. However, this subject is subject to improvement as more data becomes available. A conceptual is a representation of the current best understanding of the geothermal field, consistent with all known information and data. This model must contain enough geological, temperature, and fluid pathways within the geothermal system. This model is used to target deep

drilling and reduces the chances of test drilling risks because by the end of exploration, the field developer should provide an estimate of the field's potential to the potential financiers.

In order to make the exploration program cost effective while reducing risk, the survey design will initially focus on simpler (cheaper) methods, and become progressively more complex and costly as early results warrant more detailed efforts and project risks reduce.

A good conceptual model should provide clear evidence that the developer has integrated and considered all the collected data. The conceptual model will demonstrate a justifiable understanding of the geology, temperature, and fluid pathways within the geothermal system. By utilizing the conceptual model, the developer can select drilling sites by using all the current data. This typically involves a volumetric calculation of the heat-in-place in the project area based on a combination of:

- Estimates of the depth, thickness and porosity of possible reservoir rocks
- Known and assumed temperature distributions
- Reasonable assumptions about how much of the heat-in-place may be recovered at the wellhead

3 METHODOLOGY

This research project consists of two parts. The first part aimed at reviewing and integrating all available data and come up with a model of the geothermal system using all the known surface data. The second part involves determining the power potential of each of the discussed geothermal field and finally ranking them according to their power potential and resource characteristics.

3.1 Data collection

This project collected data and information from GDC and KenGen internal reports, Jica and BGS published reports. These companies have ownership of this geothermal fields and are in possession of the data. The data is organized in reports and some of it has been made publically available and therefore easy access. The data needed for this project included

1. Geological maps of the rock formations, structural maps, hydrogeological and volcanological studies of the volcanos.
2. Geophysical data including resistivity (MT and TEM), Gravity/magnetic.
3. Geochemical data samples for fumarole steam, water points and soil gas survey.
4. GIS data showing latitude and longitudes and also integrated with geophysical data

3.2 Data integration

The above collected geoscientific data was reviewed and integrated to come up with a raw conceptual model which is subject to improvement as more data becomes available. This model contains enough geological, thermal regime and hydrogeological regime within the geothermal system.

3.3 Power potential calculations

This project uses the power density method to estimate the resource potential. The power density method gives first-order estimates of resource capacity, expressed in terms of MW/km². This method draws a direct correlation between reservoir temperature and the MW density per surface area of the reservoir. The power found in these reservoirs is estimated using the following equation (Wilmarth et al. 2014):

Power density = 0.0528 × average temperature

Therefore

Power potential = 0.0528 × average temperature × Area.

3.3.1 Input values for the power density method

1) **Average Temperatures**

Even with the same measurement technique, temperature variations are commonly observed at different sampling locations and measurement depths at the same sampling location. Therefore, determining a single representative temperature value for the entire geothermal resource is challenging. Therefore this project gets an average temperature from the following analysis:

Upper Temperature Limit

The highest recorded well temperature in the field or the upper range of geothermometry estimates are the best choices for the upper limit of the geothermal resource, as these can indicate a higher temperature associated with a deeper reservoir zone.

Lower Temperature Limit

The following measurement outcomes, if available, can be used together to constrain the lowest likely temperature:

• The measured temperature of a shallow outflow zone

• The lower range of chemical geothermometry estimates

• The highest measured value from shallow temperature gradient wells.

After obtaining the upper and lower limit of the temperature then it becomes easier to get the average temperature by obtaining then mean.

Areal extent

Ideally, the margins of the geothermal system are determined by an inferred boundary between productive geothermal wells encountering elevated temperature and permeability and failed wells. However, this level of information from drilling does not exist during exploration phases, therefore the project focuses on the most likely areas of low resistivity, upper area limit and lower area limit to determine the area values.

Most Likely Area

Delineating the most likely extent is best determined by combining surveys of temperature with estimates for reservoir permeability. One example, if working in a high enthalpy system, is to overlap the distribution of high temperature fumaroles with resistivity surveys that correspond to an anticline of intense alteration forming a clay cap.

Upper Area Limit

The upper estimate of the reservoir area can be constrained by measurements indicating the perimeter of a zone of intensely altered clay that is consistent with a cap over upward thermal flow. If these estimates are not available for the subsurface, the surface extent of all related thermal features and associated hydrothermal alteration can be used instead.

Lower Area Limit

The lower bounds to the likely area of the geothermal system are best constrained by the extent of successful production wells. Without access to drilled wells, lower bounds can be constrained by resistivity measures around high geothermometry fumaroles, which indicate the perimeter of shallow alteration above the upflow zone of the system.

3.4 Ranking of the potential fields

After obtaining resource capacity estimates using the power density method, the geothermal fields will be ranked according to their economic value and some other social- cultural factors. The scale for the ranking will be high priority, moderate and poor. All of these fields belong to either of the three groups. Some fields are in the same group but will differ in terms of power potential. However what makes them in the same class is some factors such level of infrastructure and social economic factors.

4 RESULTS AND DISCUSION

This chapter describes in detail the resource characteristics of the undeveloped geothermal fields in Kenya. It captures the geological regime, volcanology data, geochemical data and geophysical data of each of the fields. The data is integrated to develop a conceptual model and to determine the power potential estimates of each field. The geothermal fields captured in this chapter are Suswa, Longonot, Arus Bogoria, Lake Baringo, Korosi, Silali, Namarunu, Emuruangogolak and Barrier Geothermal fields.

4.1 SUSWA GEOTHERMAL FIELD

Suswa is the southern-most caldera in the Kenyan Rift Valley. It contains a **12 x 8 km** caldera with the rim at an altitude of **1890 m**. Suswa is the closest active volcano to Nairobi, approximately 50 km north west from Nairobi and south of Longonot volcano. The Geographic coordinates are; **1.175 S, 36.35 E** and the caldera has a Summit elevation **2356 m** above sea level.

4.1.1 Volcanology

Suswa is the southernmost Quaternary volcanoes in the central Kenya rift. Earlier investigations indicated that the latest magmatic activity in Suswa is estimated to have occurred about 200 years ago within the annular trench in the caldera (Riaroh, 1994). The Phonolitic nature of the lava implies medium level magma chamber, which could provide a heat source for a geothermal system. NE-SW gravity high sitting directly on Suswa caldera suggesting a massive dense body, most likely to be a shallow magma chamber at depth of 8 km in to NE and 4 km below Ol Doinyo Nyukie. This also coincides with a reverse (‘positive’) magnetic anomaly. This could be the heat source.

4.1.2 Geology

Suswa Geothermal Prospect is associated with a central volcano with an outer and inner caldera as shown in Figure 4.1. The inner caldera has a resurgent block in the middle, which has created a circular trench around the block. The outer caldera has a diameter of about 10 km and the inner caldera has a diameter of approximately 4 km. The mountain has a maximum height of **2356m** above sea level with the caldera floor elevation of about **1900m.** Geothermal surface manifestations occurring around the outer and inner caldera where near North South structures intersect the calderas, including the trough surrounding the island block make the volcano an attractive prospect for geothermal energy investigations.

4.1.3 Geological structure

All the lava flood formations are heavily faulted trending N-S and NNW-SSE. There are acurate fault systems to the SE and SW, which may be acting as up-flows from the reservoirs.

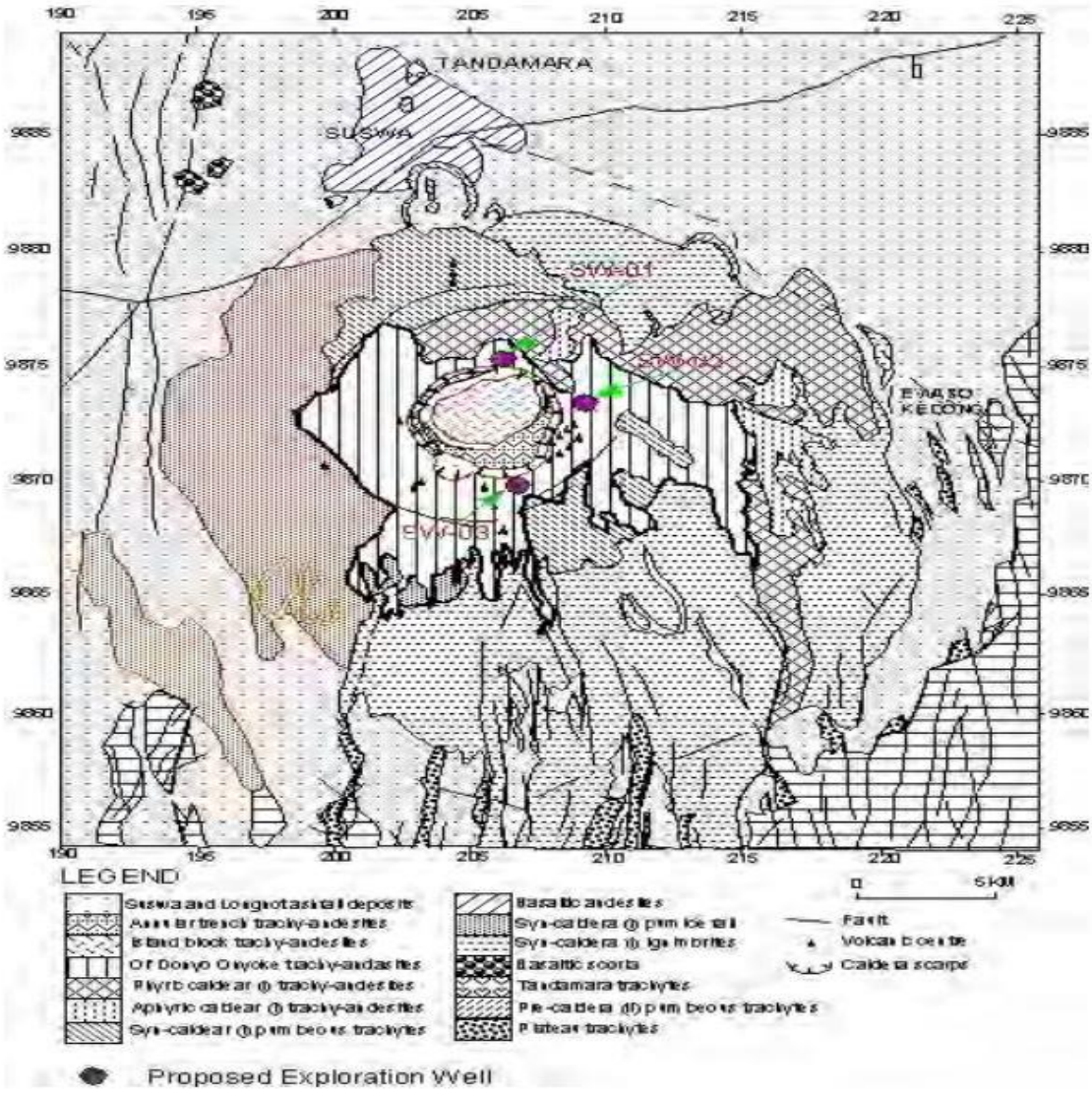

Figure 4.1: Geological map of Suswa field ((Omenda, P. A 1993)

4.1.4 Geochemistry

Geochemical studies were carried out on the fumaroles; and the waters from surface water points such as springs and rivers. These included major element chemical analyses on liquid phase samples; gas analyses on samples from fumaroles, isotopic determinations on all fluid sources in the area and soil survey have also been done. The presence of a degassing magmatic body indicates the presence of solfatara within the annular trench (Omenda, 1993). Low pH of fumarole

condensate also suggests close proximity to magma bodies or up-flow of a geothermal system (Geotermica Italiana, 1987)

4.1.5 Geophysics

Geotermica Italiana conducted interpretation of DC Schlumberger soundings in 1987 and KenGen geophysicists through MT/TEM and micro-seismic survey added Subsequent analysis.

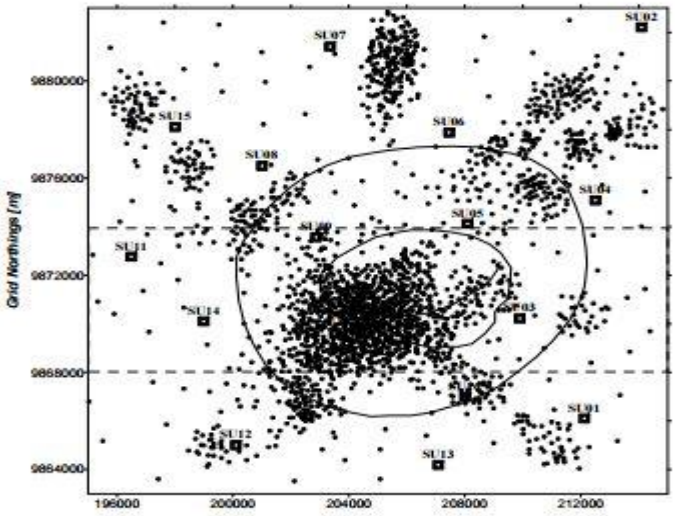

Figure 4.2: Hypocenter distribution map of Suswa field (KenGen internal report, 1987)

4.1.5.1 Gravity

A major NE-SW gravity high sitting directly on the Suswa Caldera with amplitude 250 g.u. and half wavelength of about 12.5 km in the caldera area. The anomaly appears to broaden and extend further south beyond the present area of investigation. The anomaly amplitude within the caldera is more pronounced to the south-west with its peak occurring slightly south of the Oldonyo Nyoike peak then decreases gently further south. Some small anomalies superimposed on the gravity high in the region of the Suswa caldera, which could be related to shallow structural variations and

geology within and around the caldera. Generally low gravity values trend towards the west and east.

4.1.5.2 Resistivity

Interpretation of DC Schlumberger soundings by Geotermica Italiana in 1987 as shown in Figure 4.2 and identified 3 anomalous regions of low to intermediate resistivity. The first region was found on the western half of the outer caldera extending to the south and southwest. The second region was found on the eastern slopes of the mountain with a N-S linear trend. The third region was found to NW corner of the prospect area. The results of the resistivity surveys were mapped in the Figure 4.3. The boundaries of these anomalies were not defined but appeared to cover large areas.

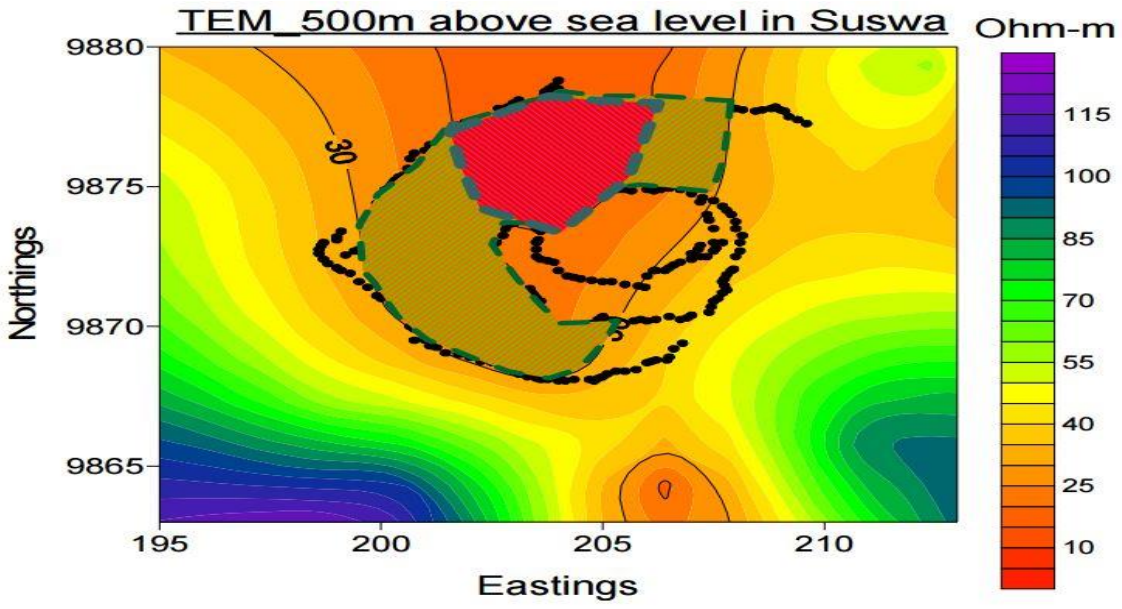

Figure 4.3: Extent of geothermal reservoir of Suswa (Geotermica Italiana, 1987)

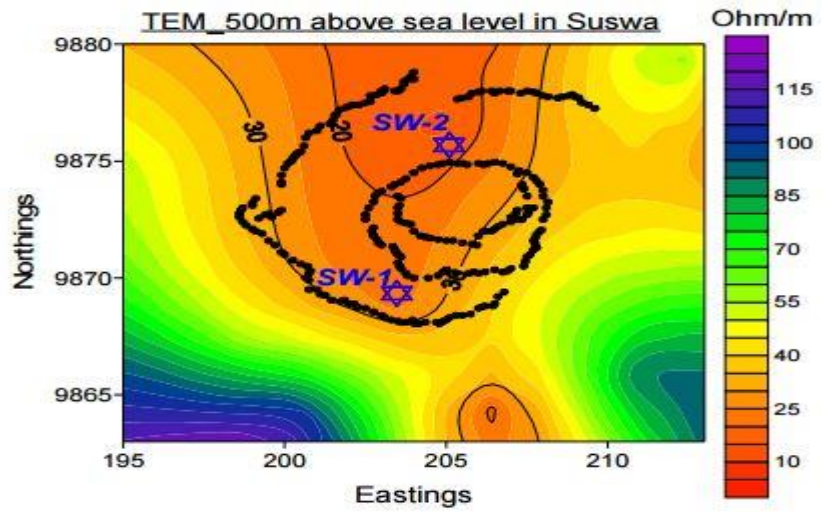

Figure 4.4: Planned points for exploratory well in the Suswa field (Geotermica Italiana, 1987)

4.1.6 Conceptual model

The geothermal system developed prior to caldera collapse as hydrothermally altered lithics occur within the syncaldera sequences. The geothermal system must have attained temperatures of more than 250℃as seen from the presence of hydrothermal epidote within the lithics. Gas Geothermometry indicate that gases sampled in the prospect originated from sources having temperatures of more than 200℃. The size of the high potential area is not well defined but is probably within the caldera floor and to the south. Resistivity data indicated that the top of the geothermal reservoir in the caldera is deeper than 1000 masl. The prospect has a good recharge from both the west and east rift escarpments. Water table is probably lower than 300 m below the floor of the valley near Suswa or greater than 600 m below the caldera floor. Recharge could be mainly from western and eastern escarpments and hydraulic gradient from the north. Further exploratory drilling has been done to understand more of the geothermal system as shown in Figure 4.4.The 2D geothermal model is represented in the Figure 4.5.

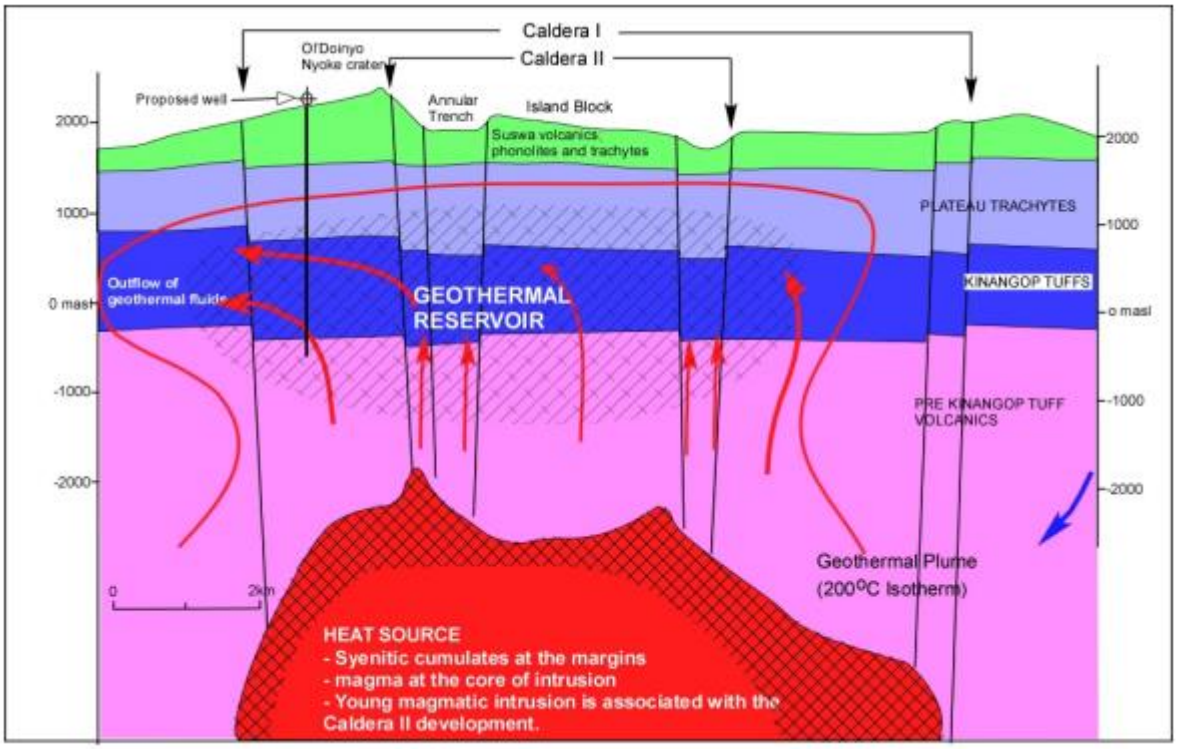

Figure 4.5: Geothermal model of Suswa volcano (JICA, 2010)

4.1.7 Power potential calculation

Average Temperature = 225 °c

Reservoir area = 30 km² - 50 km²

Power density = 0.0528×225 (°c) ＋1.7917＝ 13.6717

Power potential range = 13.6717 × 30 km² = **410 MW**

13.6717 × 50 km² = **680 MW**

In determining the power potential using the power density method, the reservoir area is assumed to be in the range of 30 km² - 50 km² and the average reservoir temperature is of 225°c, the power

density is calculated to be 13.6717 MW/km², and therefore, the resource Potential is calculated to be in the range of 410 MW - 680 MW

4.2 LONGONOT

Longonot Volcano Caldera is located east of Olkaria geothermal field on the floor of the rift valley and is bounded by the coordinates Latitudes **0°51' S** and **10°2' S** and longitudes **36°22' E** and **36°32' E.** The topography of Mt Longonot can be seen in Figure 4.6.

Figure 4.6: Site view of Longonot area

4.2.1 Geology

The Geology of the Longonot area consists of arcuate structures on the western and the southern parts, as can be seen in Figure 4.7, which mark remnants of a caldera boundary. The area in and

around Longonot is marked by active manifestations that occur in the form of fumaroles, altered grounds, warm grounds, Sulphur deposition and silica deposition. Geological studies indicate that Longonot Volcano is a Quaternary volcano, which is a divergent zone where spreading occurs resulting to the thinning of the crust hence eruption of lavas and associated volcanic activities. Trachyte, mixed basalt/trachyte, ignimbrites, base surge, pumice fall and ashes are the rock types associated with the volcano

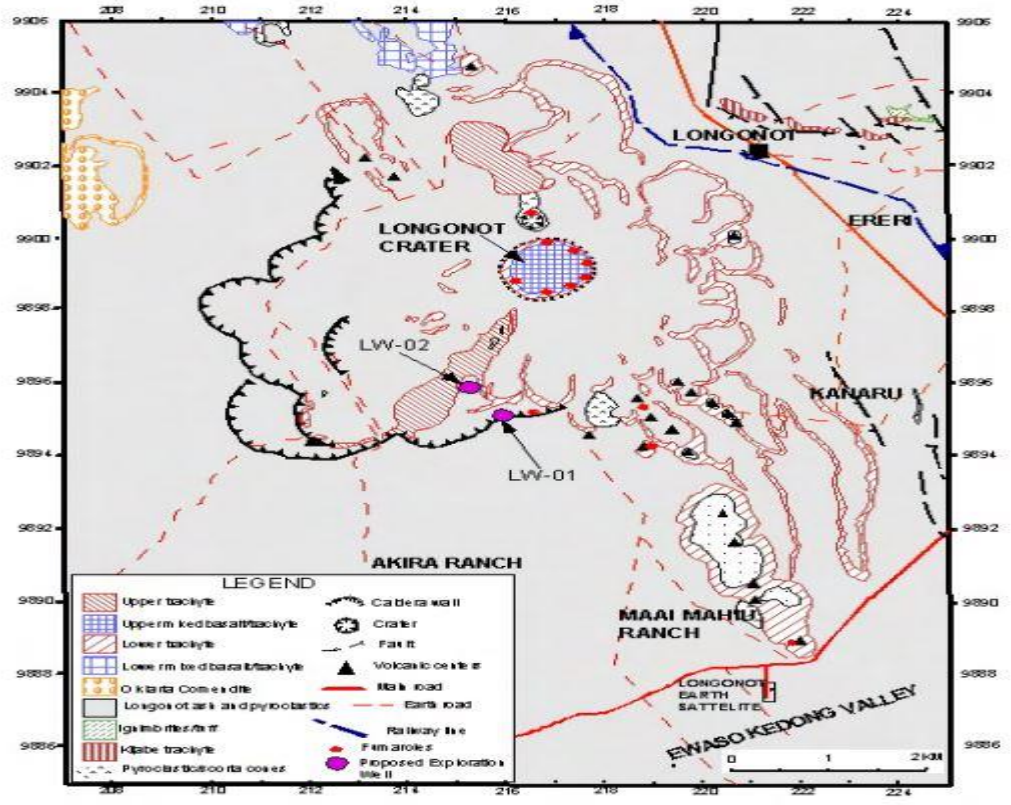

Figure 4.7: Geological map of Longonot field (Lagat, J. K., 2008)

4.2.2 Volcanology

Development of the precursor of Longonot caldera started 800,000 years ago with the development of a broad shield volcano. Volcanism continued and culminated in the caldera collapse about 9,000 years ago. Subsequent volcanism occurred in the center of the caldera and resulted in the building

of a trachytic massif and deposition of thick pumice deposits within the caldera and on the flanks. It is estimated that the most recent volcanism at Longonot occurred about 200 years ago within the summit crater and along a north-northwest trending volcano tectonic axis. There are several volcanic centers around Mt Longonot and have been mapped by various researchers such as Alexander and Ussher and they came up with map showing the various features of the crater as shown in Figure 4.8. The geothermal potential of the area is associated with a shallow magma chamber that exists under the caldera and the summit crater. A heat source in the form of shallow intrusives is postulated to exist under the caldera and the summit craters. Xenoliths showing high alteration temperatures suggest hydro magmatic eruptions encountering geothermal aquifers with high temperatures.

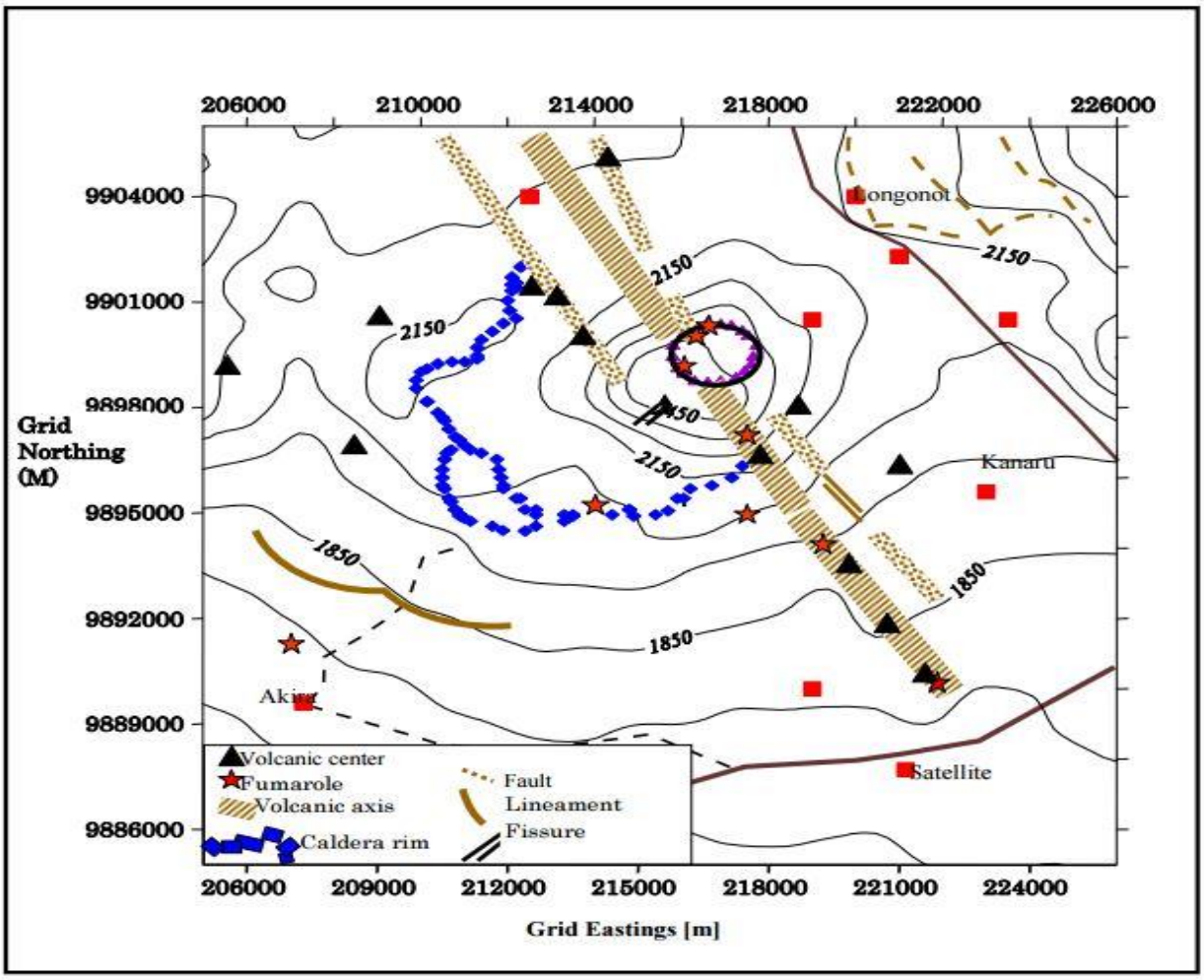

Figure 4.8: Mt. Longonot volcanic structure (Alexander and Ussher, 2011).

4.2.3 Geological structure

The main structures in the area are tectono-volcanic axis, faults, caldera rims and lineaments. The general trend of the tectono- volcanic axes is NNW-SSE and are marked by lava and pyroclastic cones, which are aligned on the northern, and the southern parts of the summit crater.

4.2.4 Geochemistry

A concerted effort was made in the 1980s to collect geochemical data. The Longonot area has limited surface activity that makes it difficult to explore using geochemical methods.

The Longonot geothermal prospect has positive indicators of a geothermal resource. Numerous manifestations occur within the summit crater and a few outside on volcanic centres to the south and on the southwestern caldera rim (Karingithi, 2005). They occur in form of fumaroles, altered grounds, warm grounds and Sulphur and or silica deposition. Few manifestations are exposed in the area due to the thick pyroclastic cover.

The few indicators include low-pressured fumaroles with a few exceptions located inside the Longonot summit crater. Geochemical survey conducted involved fumarole sampling and soil gas survey with emphasis on carbon dioxide (CO2) and radon (Rn-222) gas compositions. Reservoir temperatures estimated using the gas geothermometers indicate a resource with geothermal fluids in excess of 300°C. These are conceived to be flowing from around the main summit crater towards the south and southwest.

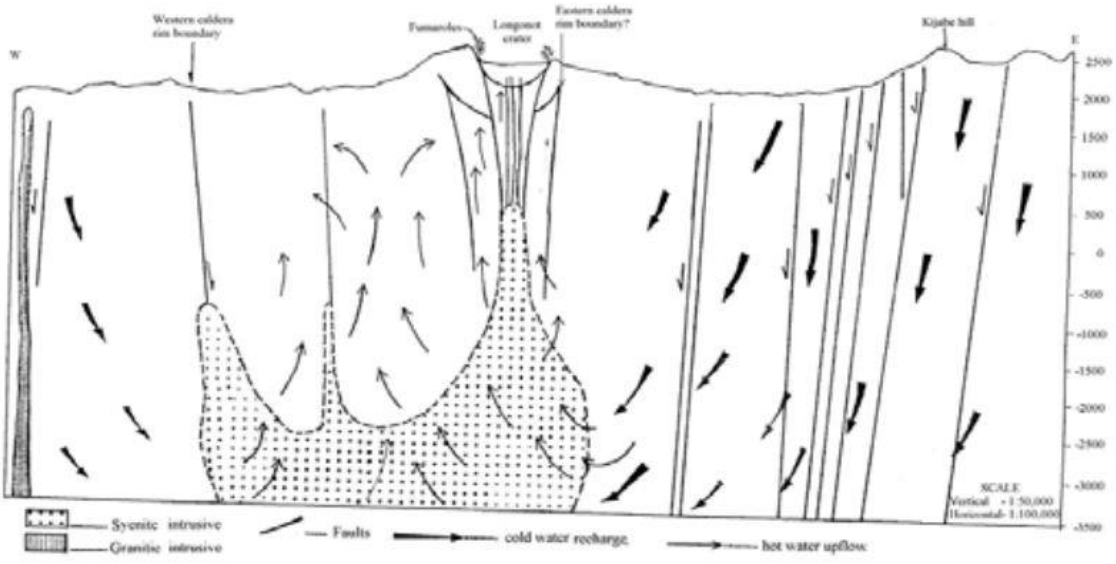

Figure 4.9: Geothermal fluid flow model of Longonot field (Karingithi, 2009)

4.2.5 Geophysics

A sizable amount of geophysics data using the gravity, resistivity and micro-seismology techniques has been collected from the Longonot prospect. A detailed interpretation of geophysical data collected by KenGen was done in the mid of 2000's, aimed at evaluating the significance of the data for sitting deep exploration wells.

4.2.5.1 Gravity

Gravity low to the north of Longonot caldera including Kijabe Hill and the north-west of it. Gravity high to the southeast. Gravity low to the west corresponding to the outer Longonot caldera. There are also localized gravity highs just north-west of Hyrax Corner.

4.2.5.2 Resistivity

Two shallow low (<10 ohm-m) resistivity anomalies were mapped. Interpretation of the data suggests a deep low resistivity anomaly exists in the area, this data is represented in Figures 4.10-4.12. The first anomaly lies to the south and southeast of the Longonot summit but within the outer caldera and covers about 70 km². It is shallower to the south of Longonot but deepens to the north. The second anomaly is found around the Akira offices further south and covers about 30 km². The northern sector of the study area shows high (>20 ohm-m) resistivity. The low resistivity anomaly is attributed to higher subsurface temperature, higher degree of hydrothermal alteration and higher permeability. The areas of higher subsurface resistivity is attributed to lower temperatures, lower degree of hydrothermal alteration and a deeper heat source. The heat source is postulated to be shallower to the south of the crater and deeper to the north as shown by MT interpretation. Geophysics data has also mapped low resistivity areas that are coincident with regional NE and NW trending faults that cut across the rift floor through the geothermal prospect. Their interpretation is that these faults control fluid flow. Combined MT, gravity and seismics indicate

that the heat source is at 6 km deep with the shallowest portion directly under the central volcano. Conceptual model indicates that the main up flow for the system is to the immediate south of the central crater extending beyond the SE margin of the caldera wall. The fluid then outflows southward. Recharge for the system is probably from the rift shoulders and also axially. The heat source for the main system is associated with the resurgent activity, which developed the central shield volcano within the caldera. The model indicates that a high temperature geothermal system >250℃ is expected to exist under Longonot. The prospect has been licensed to Africa Geothermal Investment Limited (AGIL)

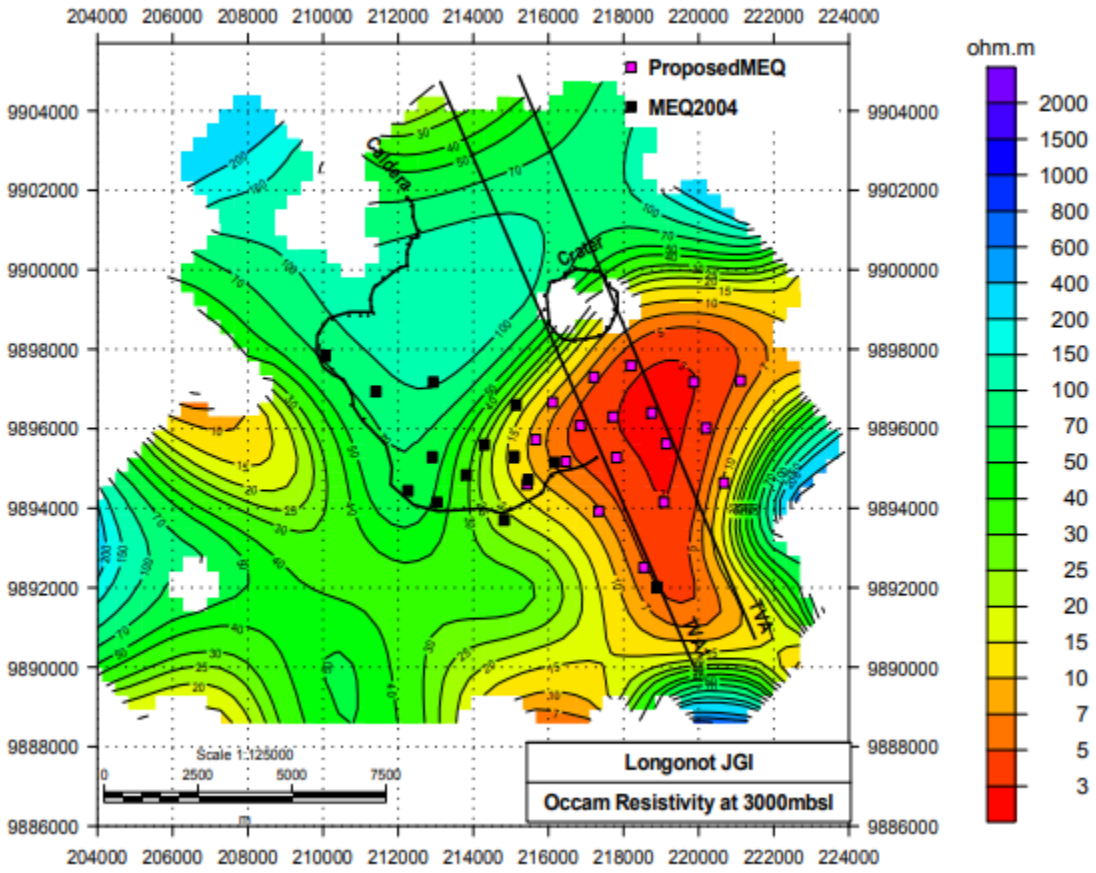

Figure 4.10: MT resistivity map of Longonot (Onacha, 2006)

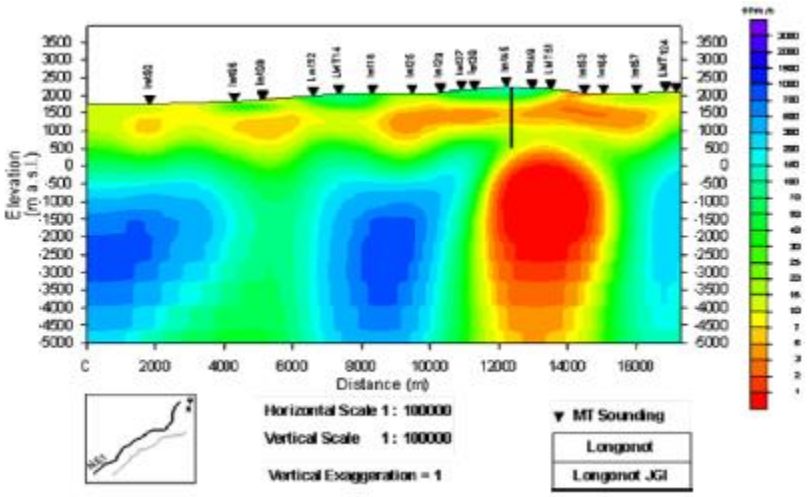

Figure 4.11: 2-D Resistivity model of Longonot Volcano ((Lagat, 2003)

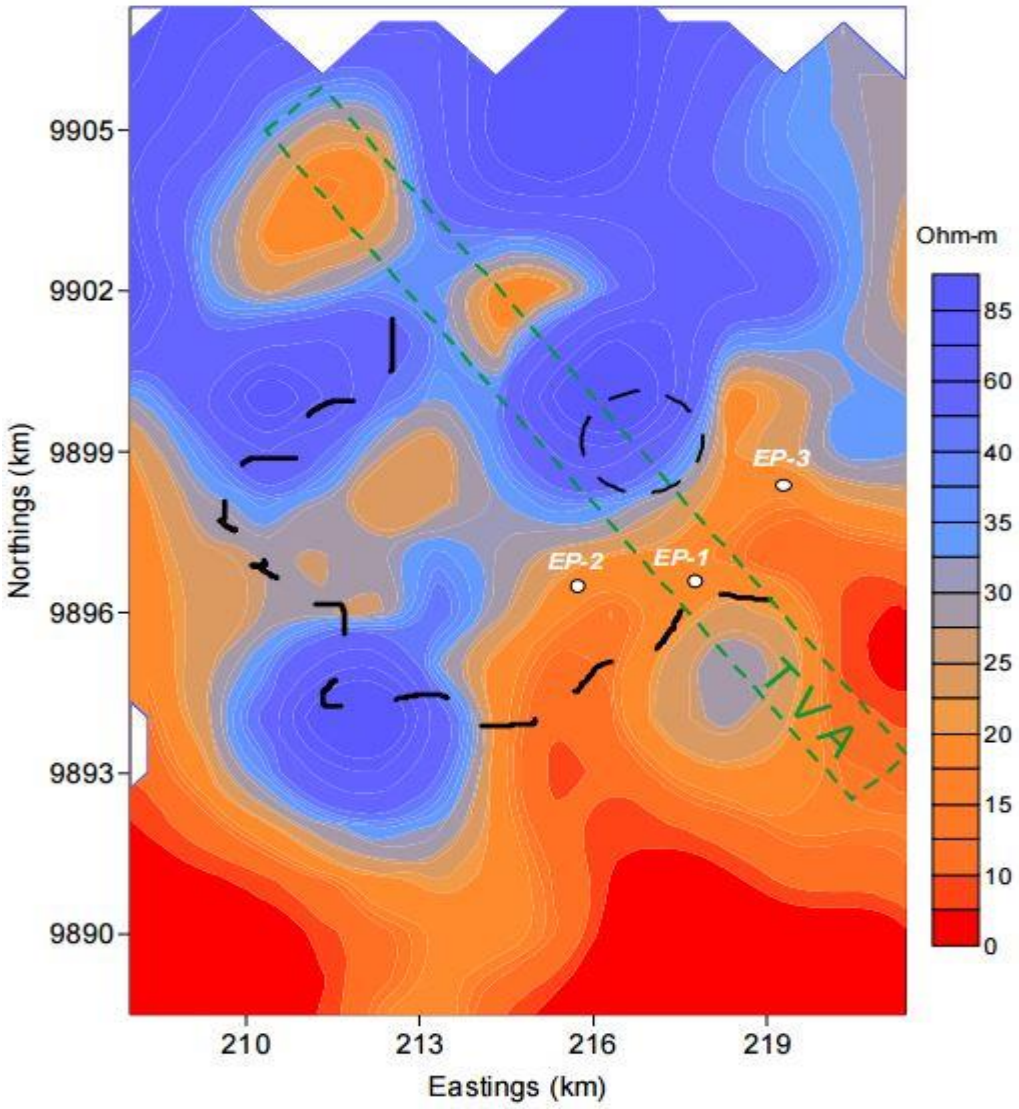

Figure 4.12: TEM resistivity map (altitude=1,300m) of Longonot field and planned well drilling site (Onacha, 2006)

4.2.6 Conceptual model

The prospect area is faulted though the faults are completely covered by the Quaternary lavas and pyroclastic from Longonot and adjacent volcanic centers. The area is most likely recharged by the flank faults from the eastern part as shown in Figure 4.9 which shows the hydrogeological model, which channel the fluids deep to the heat source. Another recharge is through the concealed rift

floor faults that run in a NNW-SSE direction, that channel the fluids from the northern part of the field. The regional hydrologic flow of the area is southwards and therefore the recharge from the north via the faults is quite possible.

4.2.7 Power potential calculations

Average Temperature =250 °c

Reservoir area = 35 km² - 50 km²

Power density = 0.0528×250 (°c) ＋1.7917＝ **14.9917**

Power potential range = 14.9917 × 35 km² = **520 MW**

14.9917 × 50 km² = **750 MW**

Using power density method to calculating the power potential of Longonot geothermal field, the reservoir area is assumed to be in the range of **35 km² - 50 km².** Assuming the reservoir average temperature of **250°c,** the power density is to be **14.9917 MW/km²,** and therefore, the resource Potential is calculated to be a range of **520-750MW**.

4.3 ARUS BOGORIA

The area referred to as Arus and Lake Bogoria prospects is located within the Kenya Rift valley immediately south of Lake Baringo prospect and north of Menengai prospect. The prospect is situated mainly within the Baringo and Koibatek Districts and includes parts of Nakuru District. The area is bound by longitudes **35°50'** and **36°10' E** and latitudes **0°00'** (Equator) **0°30' N** and is approximately 2000 km².

4.3.1 Geology

Large volumes of evolved lavas that consist mostly of peralkaline trachyte, trachy-phonolite and phonolite characterize the upper Plio-Pleistocene volcanism of the rift floor in the area between Arus and Lake Bogoria. Small outcrops of basaltic lavas occur in isolated areas within the prospect. Fluvial and alluvial deposits dominate the northern sector. The geological map of the Arus Bogoria area is shown in Figure 4.13.

4.3.2 Geological structure

The main structural features in the Arus and Lake Bogoria areas include; the eastern rift flank, the rift proper, NW, NNE and N-S trending faults and fractures and the Marigat and Loboi lineaments as shown in Figure 4.14. The most prominent of the NW trending faults is the line of Sattima-Aberdares and Marmanet Faults. Its complement to the north comprising the Lariak-North Arabel and other shorter minor faults forming a belt of discontinuous fractures. Progressively towards the northwest, both fault zones display an en echelon displacement to the west.

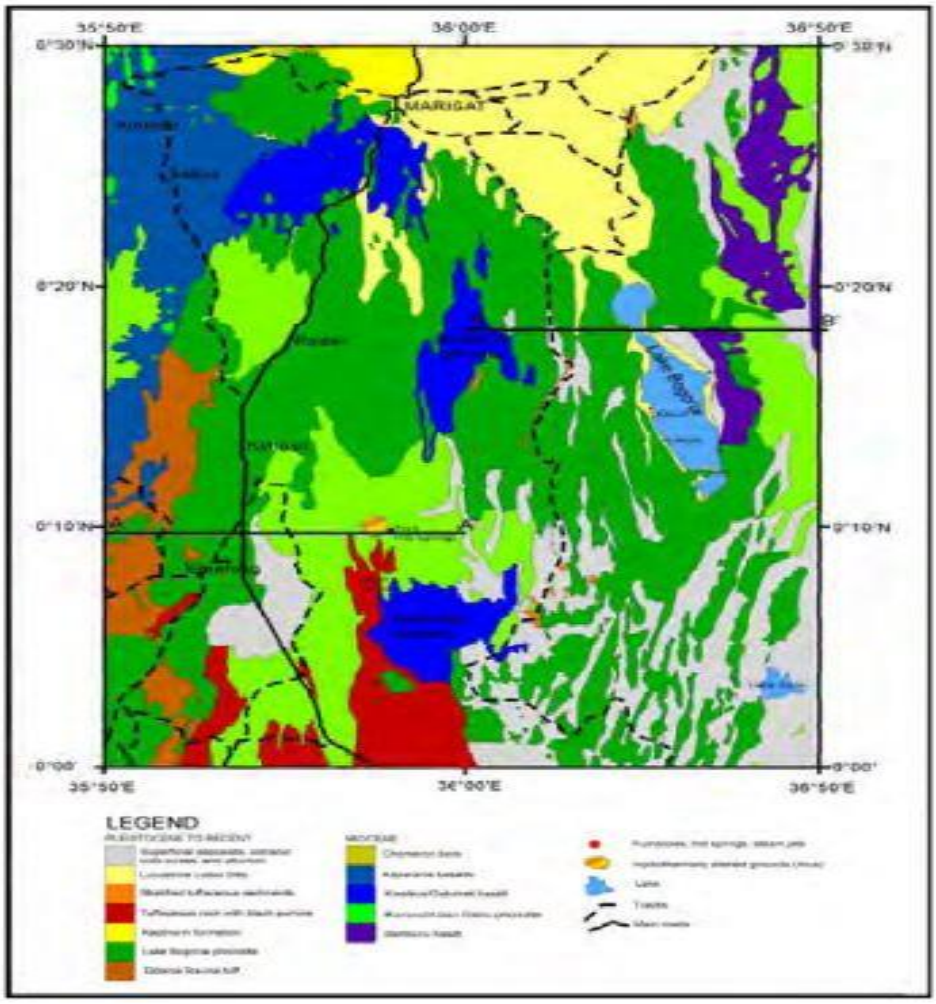

Figure 4.13: Geologic Map of the Arus-Bogoria Geothermal Prospect (Dunkley et al, 1993).

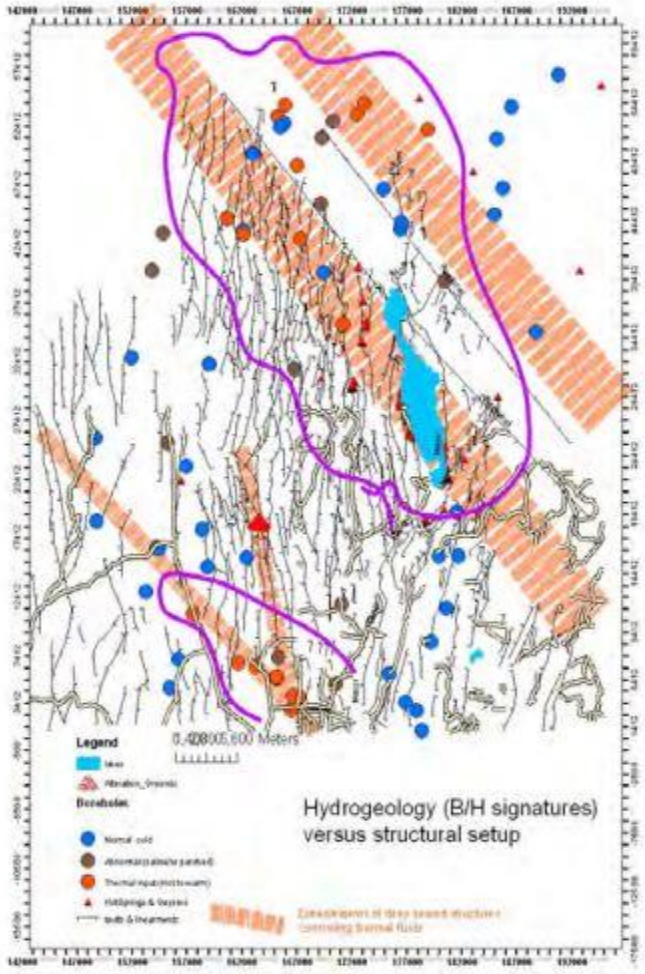

Figure 4.14: The Structural controls of the hydrogeology and hydrothermal activity in the Arus and Lake Bogoria prospect (Onacha, 2006)

4.3.3 Volcanology

Major faults extended along the western side forming half graben bounded by monoclinic flexure on eastern side and development of major basaltic-trachytic shield volcanoes occurring. Major faults developed on the eastern side with the half graben changing into full graben accompanied by basalt-trachyte volcanism. The formation of the graben structure started about 5 million years ago and was followed by fissure eruptions in the axis of the rift to form flood lavas by about 2 to 1 million years ago. During the last 2 million years ago, volcanic activities become more intense

within the axis of the rift. During this time, large shield volcanoes, most of which are geothermal prospects, developed in the axis of the rift. The volcanoes include Suswa, Longonot, Olkaria, Eburru, Menengai, Korosi, Paka, Silali, Emuruangogolak, and Barrier Complex. Other geothermal prospects, of which Arus and Lake Bogoria prospects are, occur between these central volcanoes (Omenda et al., 2001).

4.3.4 Geochemistry

Geochemical investigations of this area were carried out by Geotermica Italiana Srl, (1987) and Ministry of Energy (MOE) in 1985-1986 under the auspices of the United Nations Department for Technical Development (DTCD). The work by Geotermica Italiana covered the area from Menengai Caldera in the south to Lake Bogoria to the north. It involved sampling of water points and a few soil gas surveys targeting mainly carbon dioxide gas. The sampling points are recorded in Figure 4.16 and high flows of discharging fluids were recorded around Lake Bogoria springs and temperature estimates using solute Geothermometry from the springs and boreholes ranged from 145-190°C for borehole and spring water. Gas Geothermometry gave temperatures between 209-214oC for the Arus steam jets using CH4/H2 and CO2-CH4-CO gas functions. In the middle of 2000's, geochemical surface exploration was programmed to take one hundred and eighty working days, it was estimated to be adequate to sample all the fumaroles, springs, boreholes, and expedite soil gas surveys in the study area. The work involved:

(i) Sampling of all boreholes and springs within the Arus-Lake Bogoria prospects

(ii) Fumarole gas sampling, steam condensates and soil gas survey targeting mainly Radon-222/220 and carbon.

From the study done in the middle 2000's, geochemical exploration provides greater understanding of the location, nature and the origin of the thermal waters in a geothermal system. In addition, an insight into the recharge mechanism for the reservoir is envisaged. The information is fundamental for the assessment of the relative merits for future exploration and exploitation of a potential geothermal field. Geothermal surface activities in an area can be broadly classified into three types, which include:

(i) Hot water in form of springs and mud pools,

(ii) Steaming grounds, alteration zones and fumaroles and

(iii) Non-manifestation areas where no surface expression of geothermal activity is observed.

Figure 4.15: Hot Spring at the western edge of Lake Bogoria

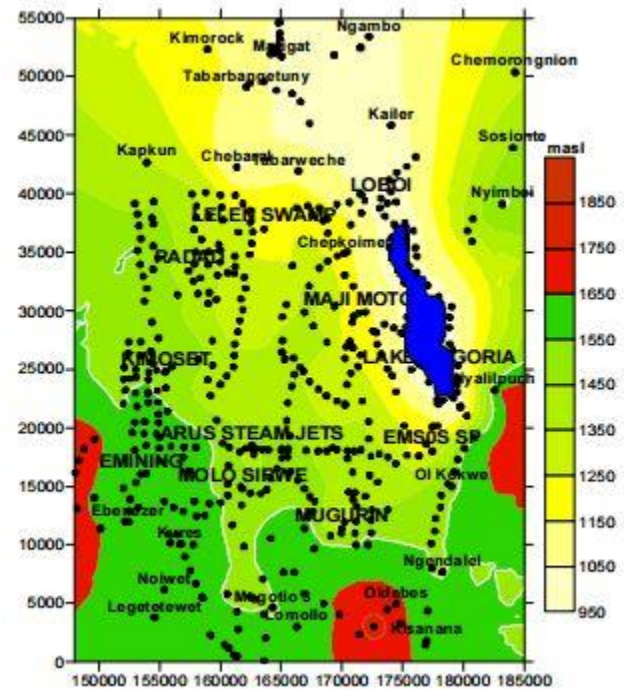

Figure 4.16: Arus-Lake Bogoria soil gas sampling points (MOE, 1986)

4.3.5 Geophysics

Since the early 1970's both passive and active source seismic investigations were applied to understand the formation and structure of the Kenyan part of the East African rift valley. The United States Geological Survey carried out seismic studies at Lake Bogoria and Olkaria in 1972 and located earthquakes of magnitude 2 or less that were restricted mainly within the fields along fault zones (Hamilton and Muffler, 1972). In 1986/87, a micro-earthquake network was setup in the Lake Bogoria region in an area of about 25 km diameter in the Molo graben, Ndoloita graben and Kamaachj horst comprising of 15 recording stations. Results from the survey appeared to suggest that most of the activity was associated with larger, older faults of the rift flanks rather than younger grid faults crossing cutting the rift. In the early 2000's, methods that were employed during exploration of Arus-Bogoria were, Magneto telluric (MT), Transient Electromagnetic (TEM) and Gravity.

4.3.5.1 Gravity

The gravity measurements were carried out using **Lacoste and Romberg gravimeter model G-767.** One hundred twenty data points were collected in the Arus and Lake Bogoria prospect. These were merged with data collected by UNDP and earlier workers for better coverage. Various plot maps of gravity were prepared from the data set comprising of over 150 gravity stations using Bouguer density of ranging from 2.0 gcm-3 to 2.7 gcm-3 using **Nettleton's method**. It was found that to get the best fit for the region an average Bouguer density of 2.5 gcm-3 had to be used.

4.3.5.2 Resistivity

TEM: A total of 47 TEM soundings, covering an area of about 1575 km2, were carried out in the Arus Bogoria prospect area using a central loop TEM array as shown in Figure 4.17. The results are presented in this report by resistivity iso-maps at various heights above sea level.

MT: An MT sounding is measured over a frequency range. The lower frequency penetrates deeper than higher frequencies. MT techniques acquire data in frequencies ranging from about 400 Hz to 0.0000129 Hz (a period of about 21.5 hrs.), and are suitable for deeper investigations. Processing, analysis and interpretation of the MT data was carried out using the computer software WinGLink and the results presented by resistivity iso-maps at various elevations and cross-sections. Results of the processed data is displayed in Figure 4.18 and from the results the Jica team prepared best drilling sites that show low resistivity anomalies(Figure 4.19).

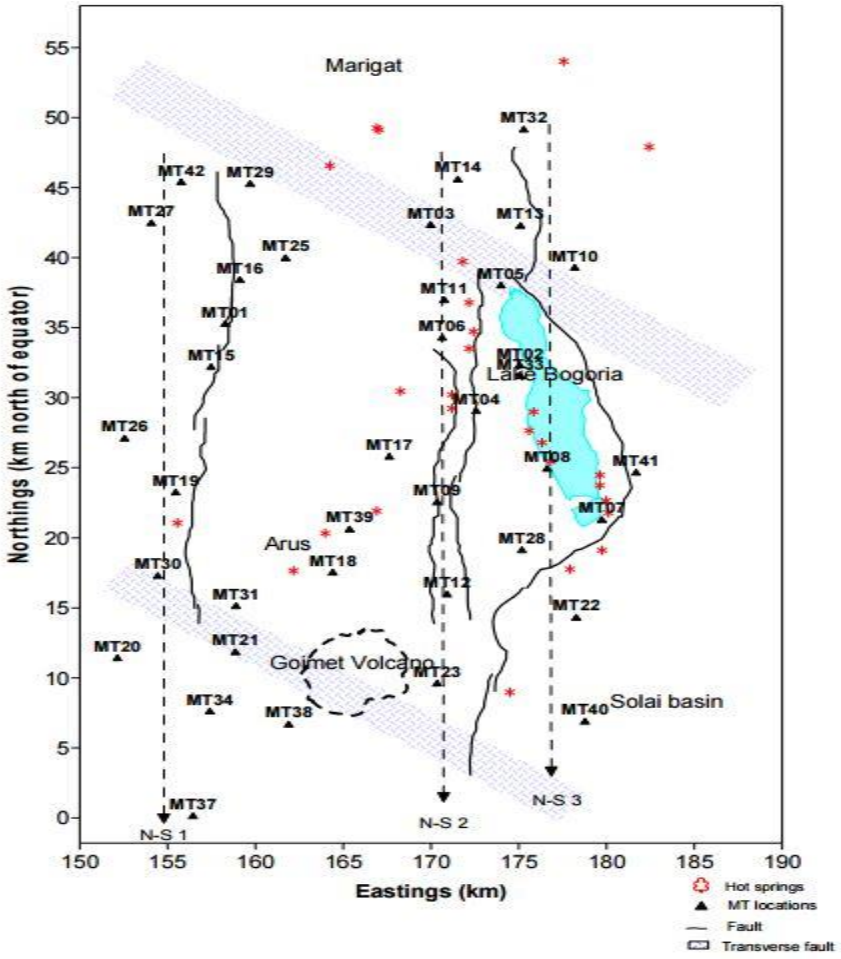

Figure 4.17: Location of MT soundings and interpreted profiles across the Arus-Bogoria region (JICA, 2010)

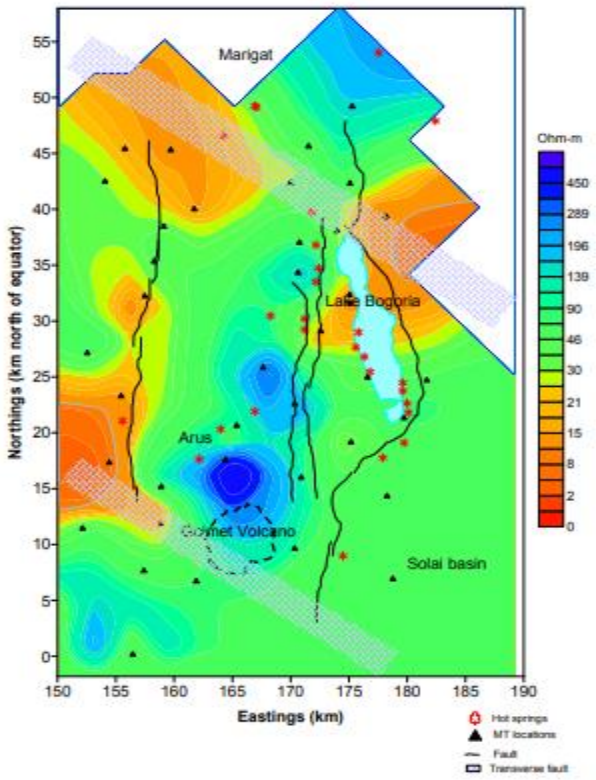

Figure 4.18: Arus-Bogoria MT resistivity distribution at 2,000 mbsl (prepared by Jica team)

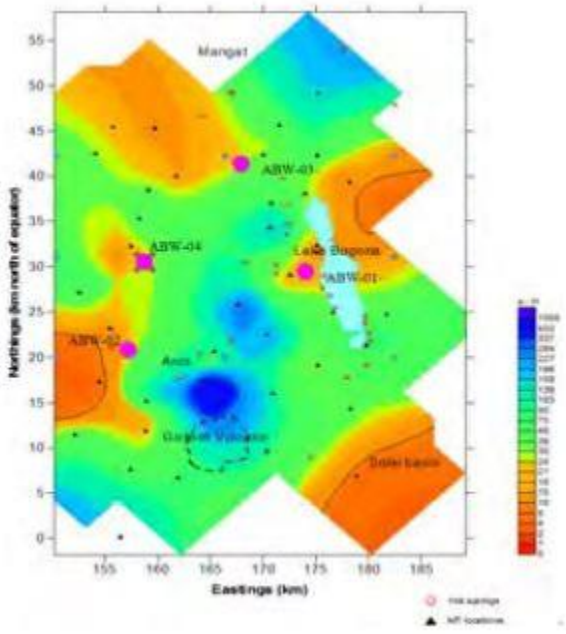

Figure 4.19: Location of Proposed Exploration Wells in Arus and Lake Bogoria prospect (prepared by Jica team)

4.3.6 Conceptual model

Fault controlled geothermal systems exist in both Arus and Lake Bogoria geothermal prospects. The estimated reservoir temperatures predicted to be medium to high (180 - 248ºC) and are ideal for electricity generation as well as direct utilization. The geothermal system around Lake Bogoria is possibly restricted to the regions around the Lake, more so the southern half. It is postulated that the geothermal system around the Lake involves deep-water circulation through the eastern and southeastern rift master faults as shown in Figure 4.20. The main recharge path would be via the Sattima-Marmanet fault system. The water would then be heated by the general high geothermal gradient in the area and localized hot bodies possibly associated with deep-seated intrusive as manifested by the occurrence of dikes on the surface. The absence of a clear centralized heat source implies that the geothermal systems are small and restricted to the fault zones. It is also postulated that the system is of medium temperature. No clear cap rock can be described for the system near Lake Bogoria.

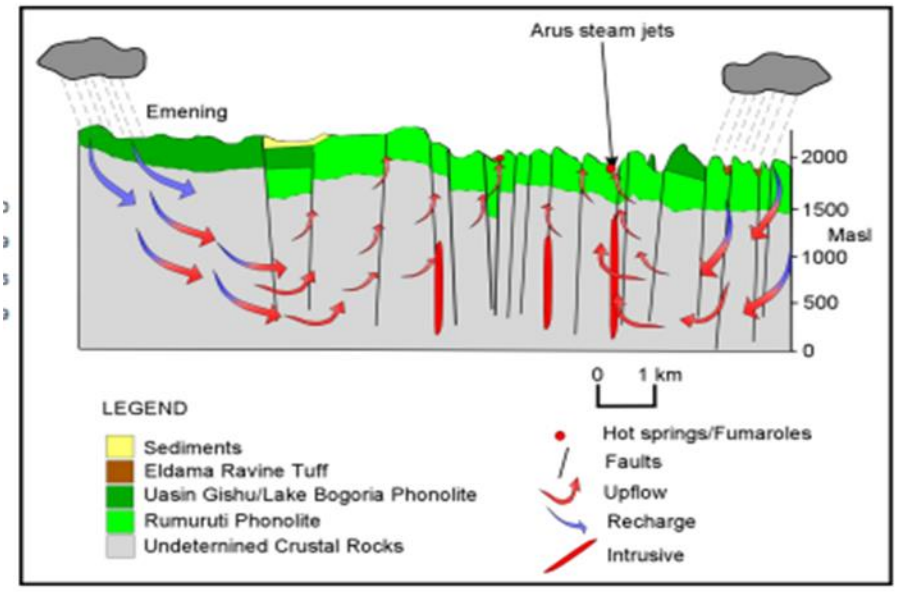

Figure 4.20: Regional geothermal model of Arus-Bogoria geothermal prospect (JICA, 2010)

4.3.7 Power potential calculations

Average Temperature – 200 °c

Reservoir area – 20 km² - 35 km²

Power density = 0.0528×250 (°c) ＋1.7917＝ **12.3517**

Power potential range = 12.3517 × 20 km² = **247 MW**

= 12.3517 × 35 km² = **430 MW**

Therefore, power potential is in the range of

247 MW - 430 MW

4.4 LAKE BARINGO

The area referred to as "Lake Baringo Geothermal Prospect" is located within the eastern floor of the Kenya Rift valley. It is bound by latitudes **0º30** AND **0º45** and longitudes **35º59'E** and **36º10'E**. Lake Baringo is a prominent feature occupying most of the central part of the area. The surface adjacent to the lake is flat to gentle N-S running grabens filled with fluvial and lacustrine deposits. N-S running sharp cliffs representing intense tectonism are also common as one moves away from the lake eastward.

4.4.1 Geology

Hydrothermal activity in the Lake Baringo prospects is manifested by extensive occurrence of fumaroles, hot spring, altered grounds and thermally anomalous groundwater boreholes. One of these boreholes, the Chepkoiyo borehole, which was drilled in April 2004, self-discharged water at 98℃(local boiling point). The chemistry of the discharged fluids indicated possible input from

a geothermal reservoir. Intermediate lavas (trachytes and trachy-phonolites) in the west dominate the geology of the area and east sectors of the prospect area and basalts in the north. The southern sector is dominated, however by fluvial and alluvial deposits. This is well illustrated in the Figure 4.21 about the rock distribution around the lake.

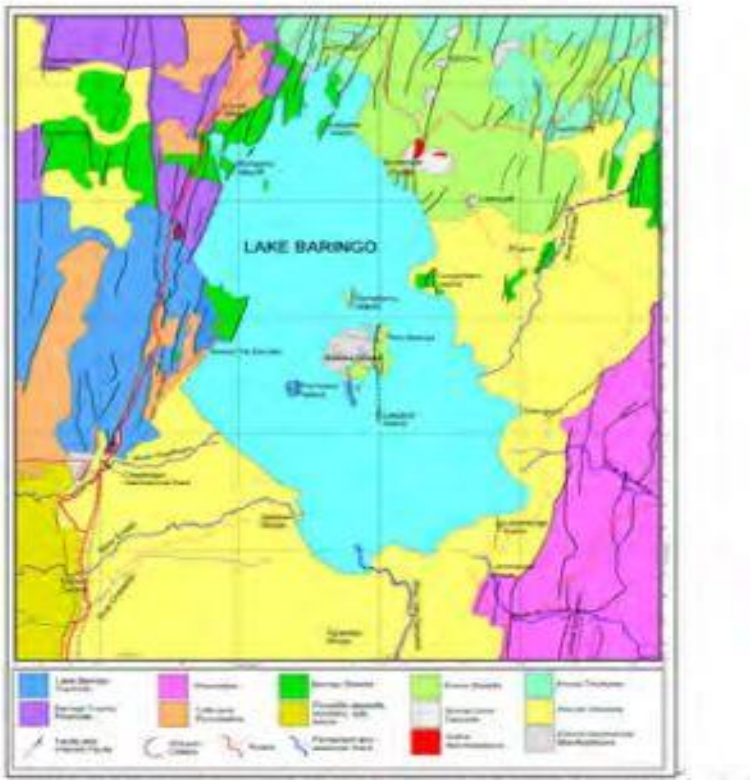

Figure 4.21: Geological map of the lake Baringo geothermal prospect. Compiled from the results of the present study and data from Dunkley et.al, (1993).

4.4.2 Volcanology

Kenya Rift International Seismic Prospect (KRISP, 1987; Henry et al, 1990) studies indicate a thinned crust comprising of volcanic material in this part of the Kenya Rift where the prospect area

is located. The heat source for this system is most likely dike swarms associated with the faults along which repeated fissure eruptions have taken place.

4.4.3 Geologic structure

The structural pattern of the Lake Baringo area is complex due to interaction between the old and young fault systems in the area. The dominant structure in the prospect is the young N to NNE trending fault pattern that form a dense fault swarm restricted to the rift axis. Within the prospect, the faults dip west and east for those to the east and west of Lake Baringo, respectively. The main faults in the prospect have dips of up to 100 m. Figures 4.22 and 4.23 show the geological structure and stratigraphic cross- section of the rocks between east and west of the lake Baringo.

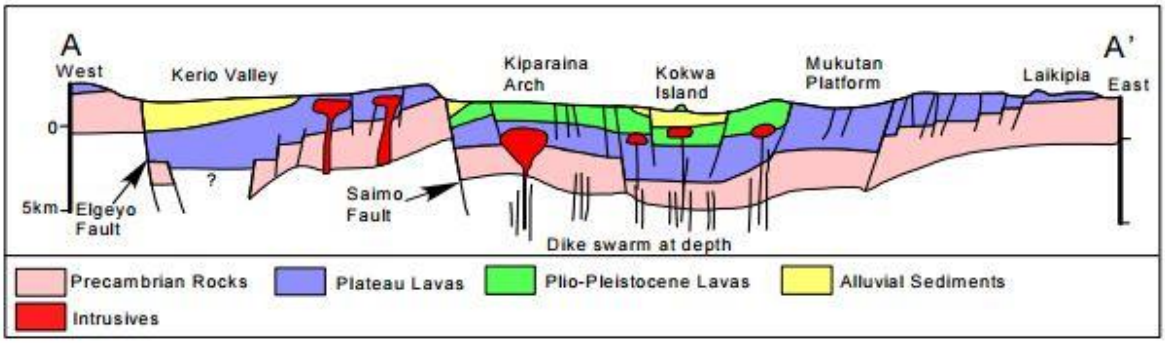

Figure 4.22: Generalized Litho-Stratigraphic Cross Section through Lake Baringo Geothermal Prospect (MOE, 2004)

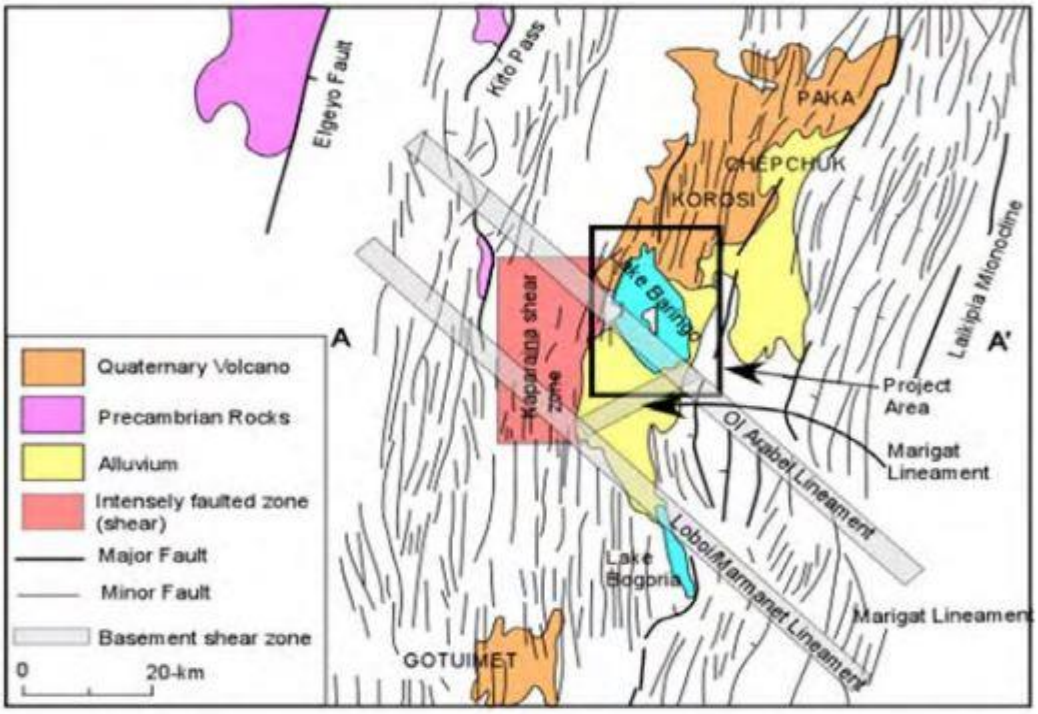

Figure 4.23: Structural map of the area around Lake Baringo Geothermal prospect. Major (Precambrian?) lineaments (Shear zones)

4.4.4 Geochemistry

Figure 4.24 shows the few sampling points that consisted of fumaroles and boreholes, soil gas and Radon-222 surveys that were conducted throughout the prospect between June 2004 and August 2004. Gas geothermometers recorded temperatures of 168°C to 310°C calculated using CO2, H2 and solute Na/K/Ca. High radon counts and high CO2 measured in the soil gas were observed around Loruk, the area west of Kampi ya Samaki, Rugus and southeast of Kiserian and could be indicative of enhanced permeability in these areas.

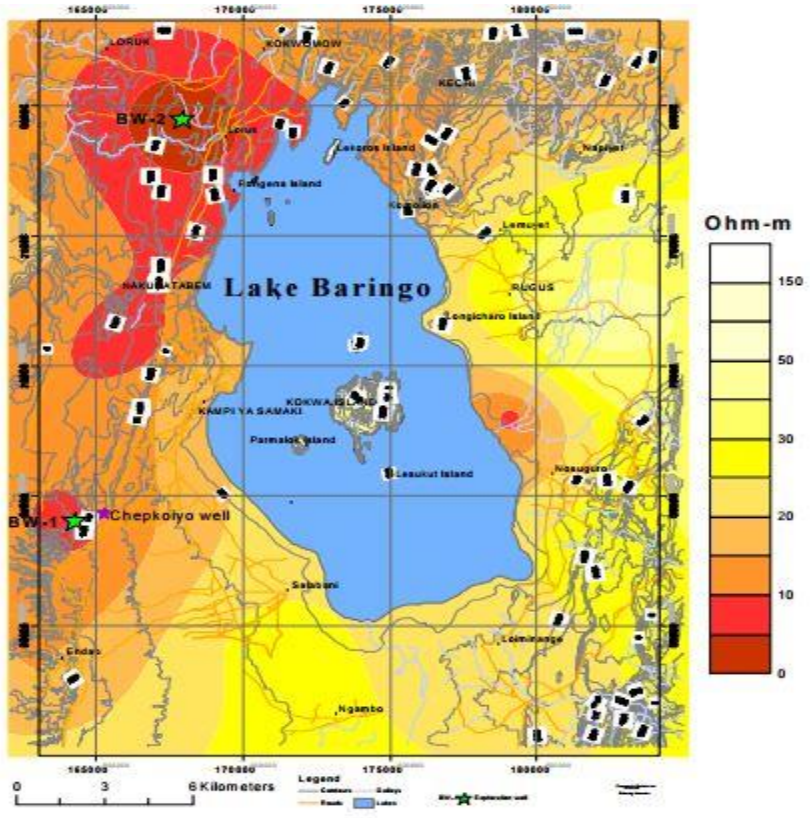

Figure 4.24: Geochemical sampling points for the Lake Baringo prospect (MOE, 2004)

4.4.5 Geophysics

A geophysical survey comprising of gravity, ground magnetics, MT and TEM methods was carried out between May and June, 2004 in order to investigate the thickness of the sedimentary basins and the anticipated underlying volcanics, identification of structures that could be possible conduits for geothermal fluids and presence of heat sources. Schlumberger resistivity done by MOE in the late 1980s A few gravity measurements done by universities in the early 1990s. Aeromagnetic data collected by the National Oil Corporation of Kenya in 1987 and Micro-seismic monitoring to the south of Lake Baringo carried by the University of Leicester in the early 1990s.

4.4.5.1 Gravity and magnetics

Gravity: Gravity highs are seen on higher altitudes along the northern and eastern flanks of the area, i.e., Korosi and the S-E of Lake Baringo as shown in Figure 4.25. Other high gravity areas are those associated with volcanics appearing on the surface to the west near Loruk and Kampi Ya Samaki. A gravity high is seen to the S-W of the lake and runs approximately N-S, passing through the Chepkoiyo well and coincident with the fault along Marigat-Loruk road. Incidentally, the geothermal manifestations appear on these volcanics. A trend of gravity lows is seen running in a NE-SW through the southern part of the lake. The lowest gravity signal was recorded south of Lake Baringo on fluvial sediments.

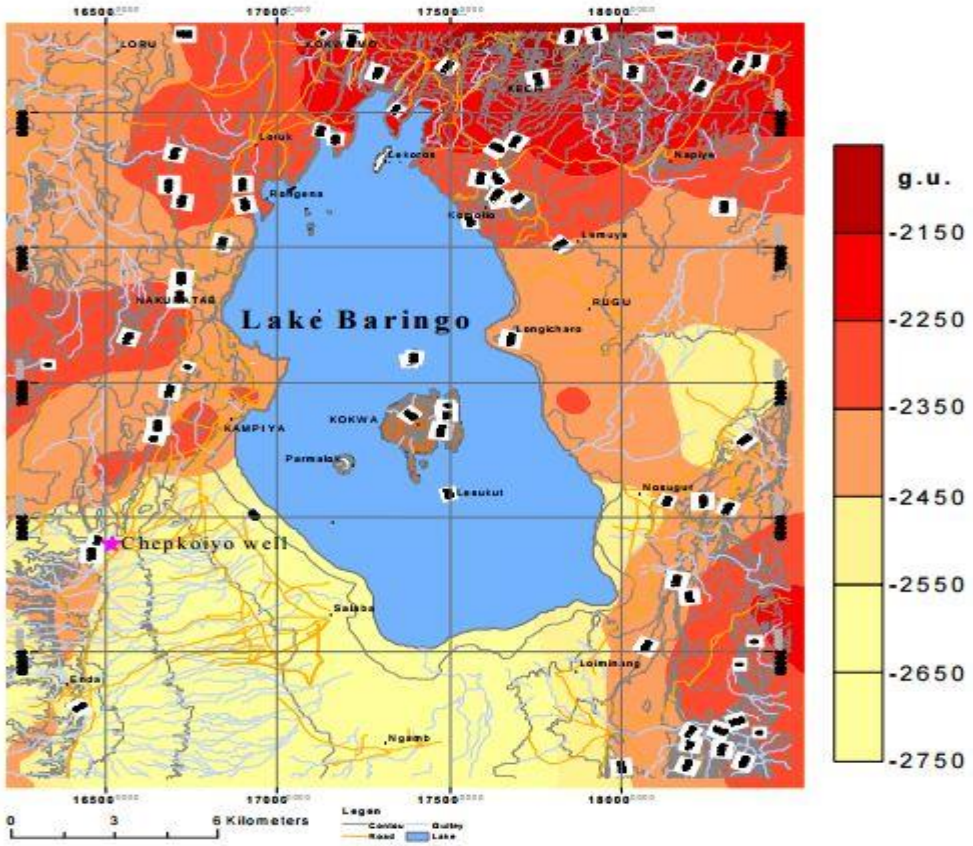

Figure 4.25: Bouguer Anomaly Distribution in the Lake Baringo Geothermal Prospect (KenGen 2004)

Magnetics: The highest magnetic signal was recorded at the southeastern slopes of Korosi, around Komolion, NNE of the survey area. The lowest values are seen on the sediments around the lake. The region around Chepkoiyo well has signals of moderate values. Generally, the magnetic signatures in the western sector trend in a N-S direction and tend to mimic that of low resistivity at 500 masl.

4.4.5.2 Resistivity

TEM: At the elevation of 500 masl, it is observed that these resistivities are in most areas lower than 20 ohm-m for all the depths investigated. A trend of low resistivity (<5 Ohm-m) is seen running in an N-S direction west of the lake passing through the Chepkoiyo well, see Figure 4.26. The other such low resistivity trends in an NE-SW direction through the Chepkoiyo well, Ol Kokwa Island and Rugus hills to the NE. Slightly higher resistivities (8-20 Ohm-m) exist to the south, north, N-E and further west of the lake.

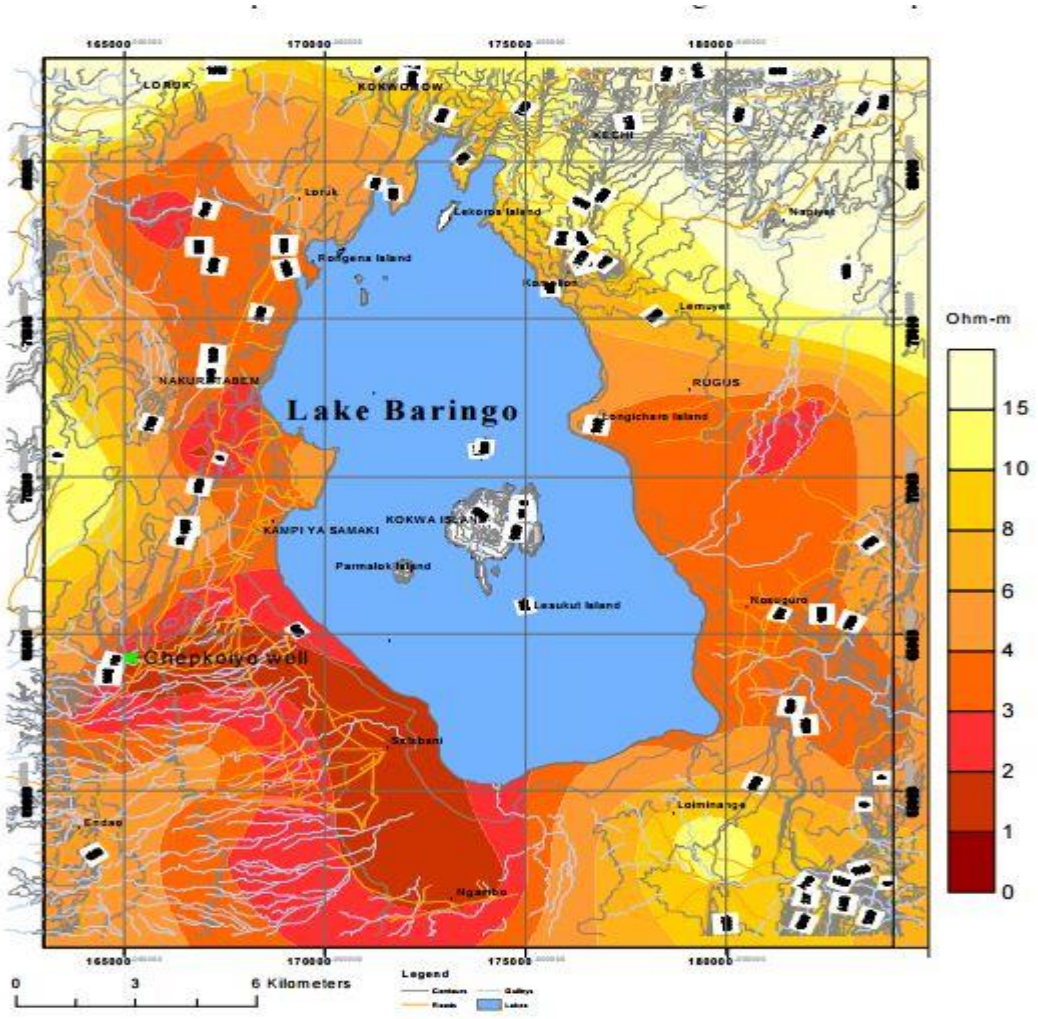

Figure 4.26: Resistivity Distribution at 500masl from TEM measurements in the Lake Baringo Geothermal Prospect (KenGen 2004)

MT: Planar resistivity variations of MT data at sea level, 2000 masl and 5000 masl, respectively. At the near surface, these anomalies mimic those of TEM in most areas around the lake (Figure 4.27). Low resistivity anomalies exist to the west, NE and SE of the lake. The shapes of the low anomalies also tend to follow the topography due to sediment deposition. Tongue et al. (1994) have also derived similar information from seismic experiments. At deeper levels, the western low resistivity anomaly persists, spreading out to the north and northeast.

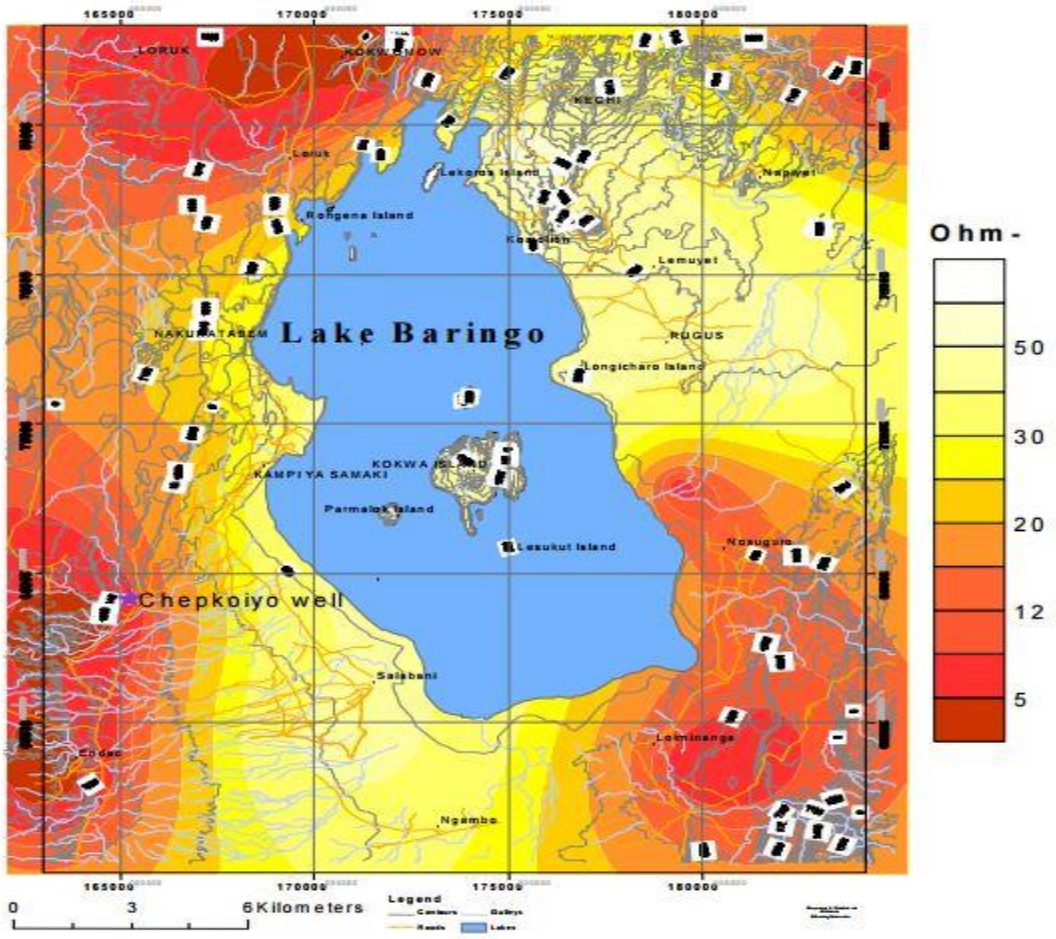

Figure 4.27: Resistivity Distribution at sea level from MT measurements in the Lake Baringo Geothermal Prospect (KenGen 2004)

4.4.6 Conceptual model

- Geoscientific data indicate existence of a geothermal resource in Lake Baringo prospect, which is characterized by intermediate to high temperatures. Scientists from GDC have come up with a 2D conceptual model of Lake Baringo geothermal system and is shown in the Figure 4.28.
- The heat source for the geothermal systems are dyke swarms and shallow intrusive bodies associated with faults and the reservoir rocks are the Plio-Pleistocene lavas.

- Gas geothermometers recorded temperatures of 168°C to 250°C calculated using CO2, H2 and solute Na/K/Ca.
- High radon counts and high CO2 measured in the soil gas were observed around Loruk, the area west of Kampi ya Samaki, Rugus and southeast of Kiserian and could be indicative of enhanced permeability in these areas.

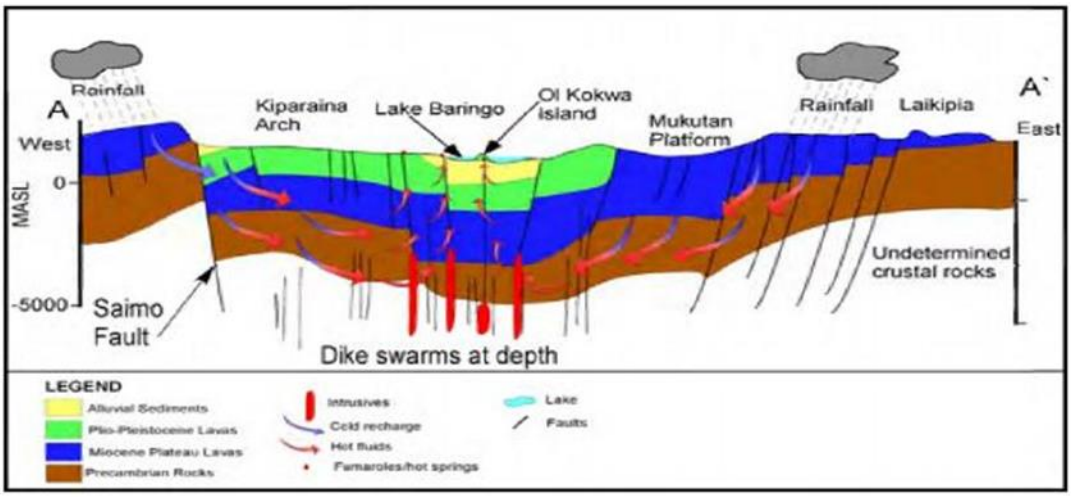

Figure 4.28: Simplified Geothermal Model of Lake Baringo Geothermal Prospect (Adapted from GDC internal reports)

4.4.7 Power potential calculations

Average Temperature = 200 °c

Reservoir area – 20 km² - 25 km²

Power density = 0.0528×250 (°c) ＋1.7917＝ 12.3517

Power potential range = 12.3517 × 20 km² = **247 MW**

= 12.3517 × 25 km² = **308 MW**

4.5 KOROSI

Korosi - Chepchuk area is located in Baringo district of the Kenyan Rift Valley and is neighboring Lake Baringo to the south and Paka volcano to the north at approximately 00o 45'N, 36o05' E. The volcano occupies an area of about 260 km2 and rises to about 500 m above the surrounding floor of the inner trough of the rift valley, reaching a maximum height of 1446 M on the summit cone of Kotang in the northeast.

4.5.1 Geology

The geology of Korosi is mainly dominated by the intermediate lavas (trachytes and trachy-andesite), which cover the central and eastern sectors of the prospect area and basalts dominating the south, north and western sectors. The southwestern plain is, however, dominated by fluvial and alluvial deposits whereas the air-fall pumice deposits dominate the western plains. A clear representation of the geology of Korosi area is shown in Figure 4.29.

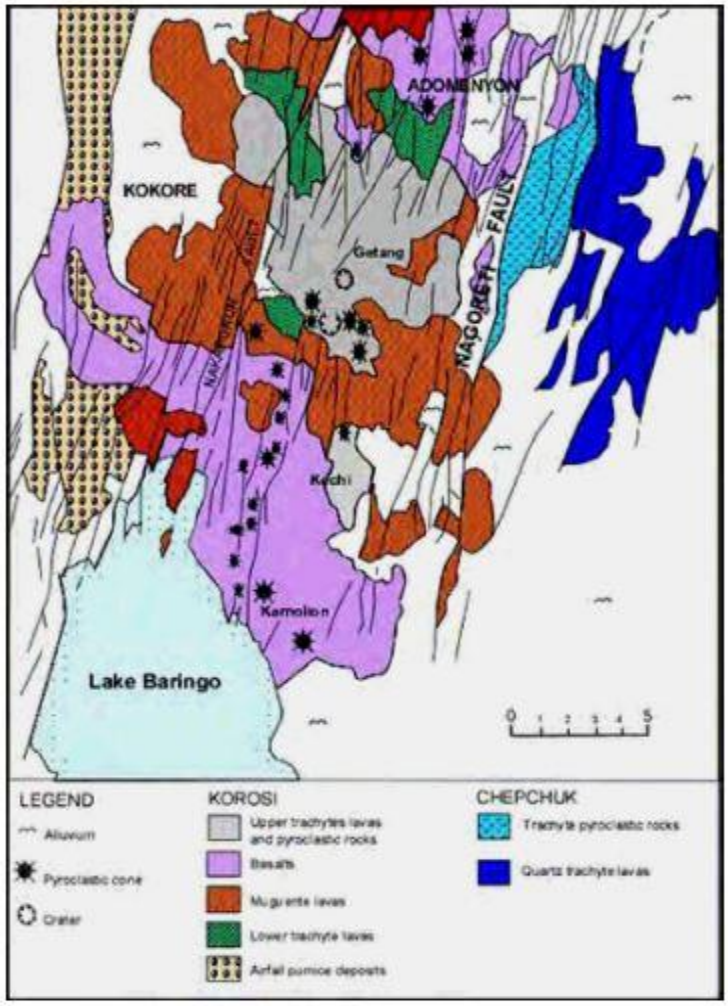

Figure 4.29: Geological map of Korosi - Chepchuk area (Dunkley et al, 1993)

4.5.2 Volcanology

Korosi is a multi-vent complex composed predominantly of trachyte lavas, which have built up a low volcanic shield, upon which lesser amounts of basalt, mugearite and pyroclastic deposits have erupted. The main faulting and basaltic activity were followed by the eruption of Upper Trachyte lavas, domes and pumice scoria cones, which are aligned along the NNE-trending faults. The majority of the lavas were erupted from the northern part of the summit area and flowed down to the northern flanks of the volcano. Radiometric dating of the Upper Trachyte lavas indicates an

age of 104±2 Ma. Heat source is associated with shallow magmatic bodies under the volcano and intrusive dykes along NNE structures. The location of the prospect areas allows for recharge of waters from the wet rift flanks into the deep hot intrusives. The areas have extensive faulting which can allow upflow of hot geothermal fluids to shallow depths.

4.5.3 Geologic structure

The structural development of the Korosi segment of the rift occurred between 5.3-1.6±0.01 Ma with the landscape as it is today having been formed during the last 100,000 yrs BP. The structural setup of the area is defined by dominant NNE and N trending fault swarm within the axial region, as seen in Figure 4.30. The dominant fault trend at Korosi is somewhat discordant with rift boundaries at that latitude which is more in NE trend. The fault zone defines a micro-graben within the axis of the rift; the boundaries of which are marked by the Nakaporon fault in the west and Nagoreti fault in the east. The latter fault also defines the western boundary of the Chepchuk volcanic edifice. The Korosi volcanic massif is located entirely within the micro-graben marked by the Nakaporon and Nagoreti faults but with a bias to the west resulting in some of the Korosi volcanic products overflowing the walls of the east-dipping Nakaporon fault. The occurrence of cinder cones and other volcanic centres are controlled by the major N and NNE trending faults.

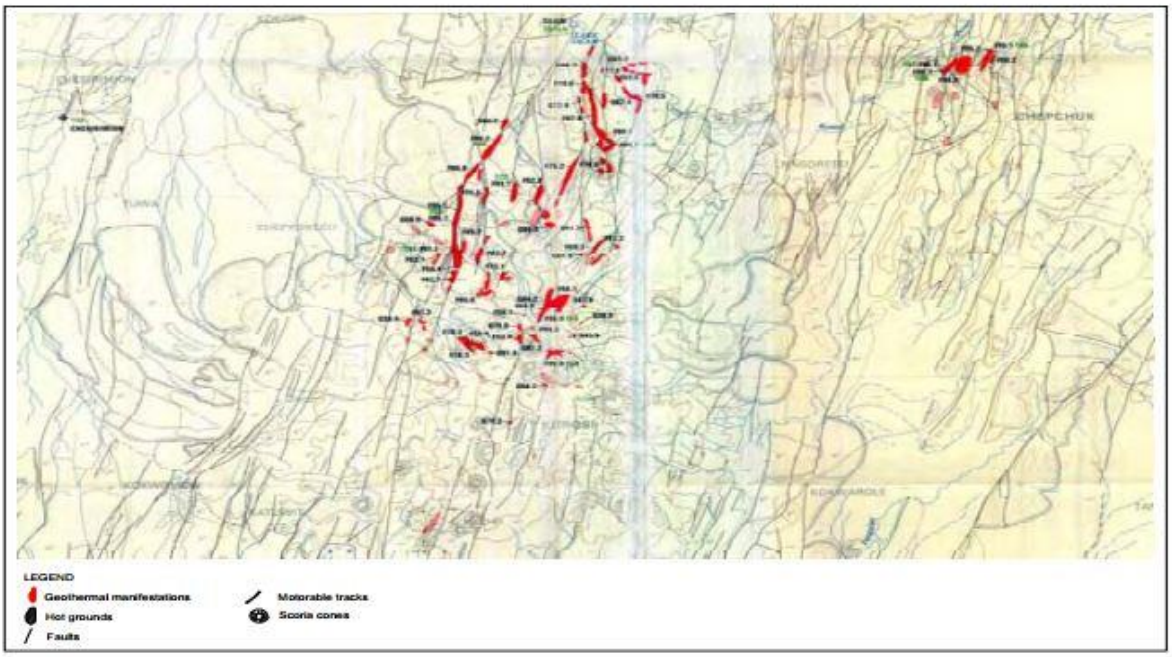

Figure 4.30: Structural map of the Korosi Geothermal Prostect indicating areas of high thermal manifestations ((Kengen,2006)

4.5.4 Geochemistry

Fumarole steam chemistry indicate reservoir temperatures in the range of 200- 280 oC for both Chepchuk and Korosi prospects calculated using gas based geothermometers (TH2S). The fumaroles with the highest calculated Geothermometry temperatures are found around Chepchuk (209℃ – 282 ℃) and around Korosi (244℃ – 259℃).

4.5.5 Geophysics

Gravity and Ground Magnetic surveys, Transient-Electromagnetic (TEM) measurements, Magnetotellurics (MT) measurements and Micro-Seismic data collection were carried out in KenGen surface exploration study (2005-2006). 44 TEM soundings, 36 MT soundings, 280 Gravity stations and 280 Ground magnetic stations were covered. Results of these investigations

have been used to infer the depth and extent of the possible heat source and geothermal reservoir and site the exploration wells.

4.5.5.1 Gravity and magnetics

Aeromagnetic data exist over much of the Kenya rift valley. The data was collected by CCG for the National Oil Corporation of Kenya (NOCK, 1987). These data were examined along with gravity anomalies and a qualitative interpretation carried out over the Korosi-Chepchuk prospects. Magnetic anomalies seen here were not different from those over those coinciding with volcanic centres at Suswa, Olkaria, Eburru and Menengai. These anomalies are interpreted as being caused by changes in the susceptibility of rocks due to demagnetization by heating above the Curie point. It is observed in Figure 4.31 that, both from gravity and magnetic data that an anomalous area exists in the central part trending in a NE direction, connecting the volcanic centres of Korosi, Chepchuk and Paka. The gravity and magnetic signatures suggest shallow magmatic intrusions (Figure 4.32). These could be providing the heat source to possible geothermal reservoirs. The data shows that there could be a large resource in the western and north-western parts of the prospect.

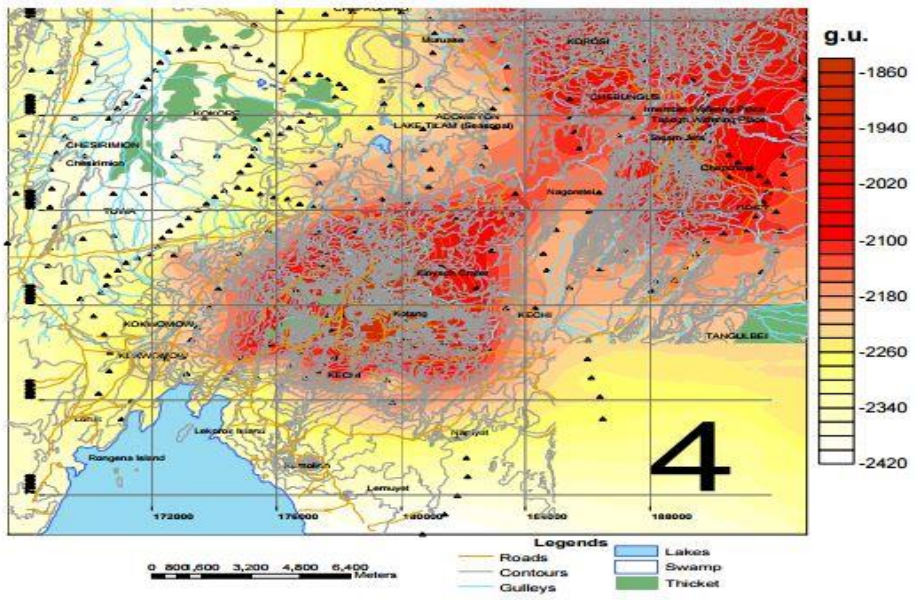

Figure 4.31: Bouguer Anomaly Distribution in the Korosi - Chepchuk area. The triangular symbols indicate the locations of the gravity stations. (JICA, 2010)

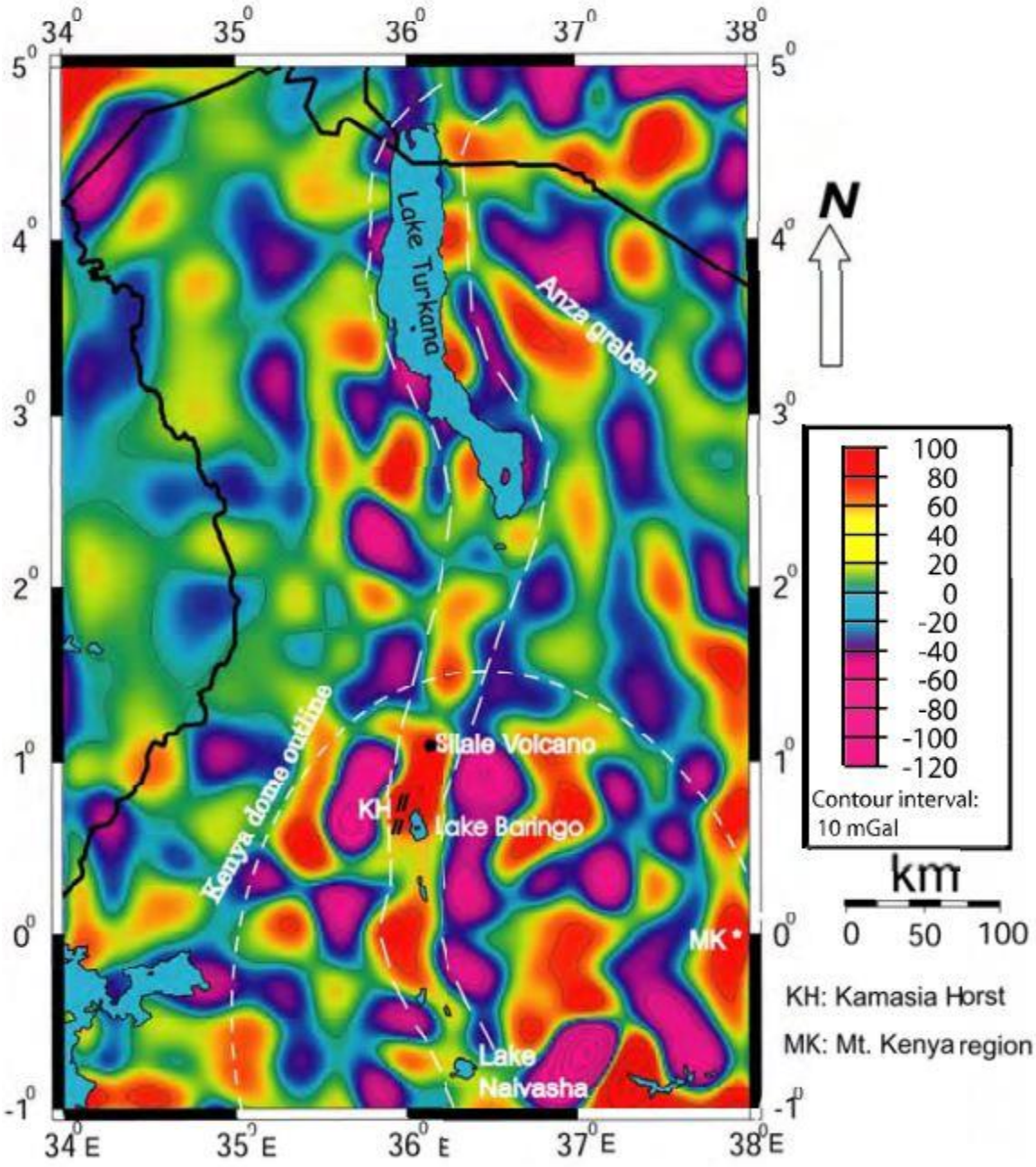

Figure 4.32: Band- pass filtered gravity map of the northern part of the Kenya rift. (Mariita, 2003)

4.5.5.2 Resistivity

From the resistivity results from TEM and MT suggest that the Korosi-Chepchuk prospect appears to host three large geothermal systems occupying the immediate NW of Lake Baringo (near Loruk center), NW of Korosi massive and NE of Chepchuk volcano (Figure 4.34). Intersections of major

structures such as Ol Arabel lineament with the NE-SW and N-S structures that run along the rift floor appear to play a significant role on resistivity distribution in this prospect. MT resistivity cross-sections show low resistivity anomalies at depth that could be related to heat sources (Figure 4.33).

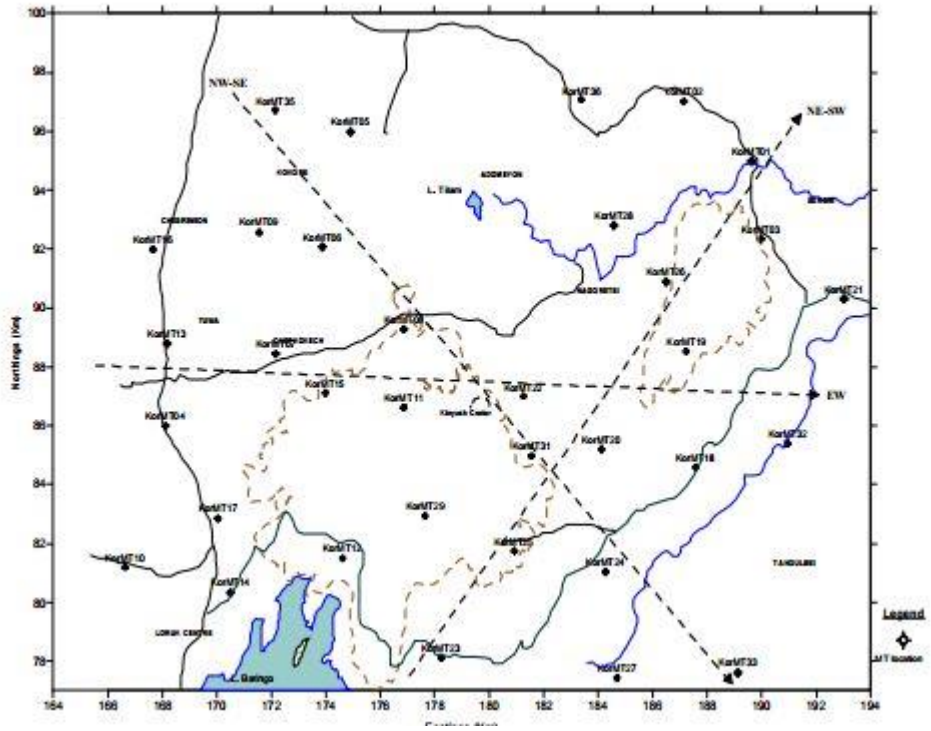

Figure 4.33: MT stations of Korosi - Chepchuk Prospect (Kengen,2006)

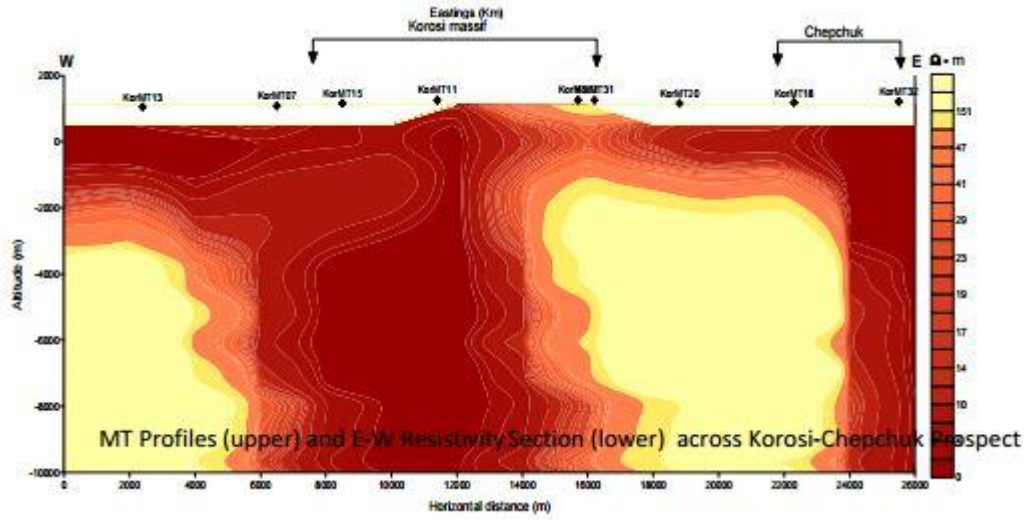

Figure 4.34: MT Profiles (upper) and E - W Resistivity Section (lower) across Korosi - Chepchuk Prospect (JICA, 2010)

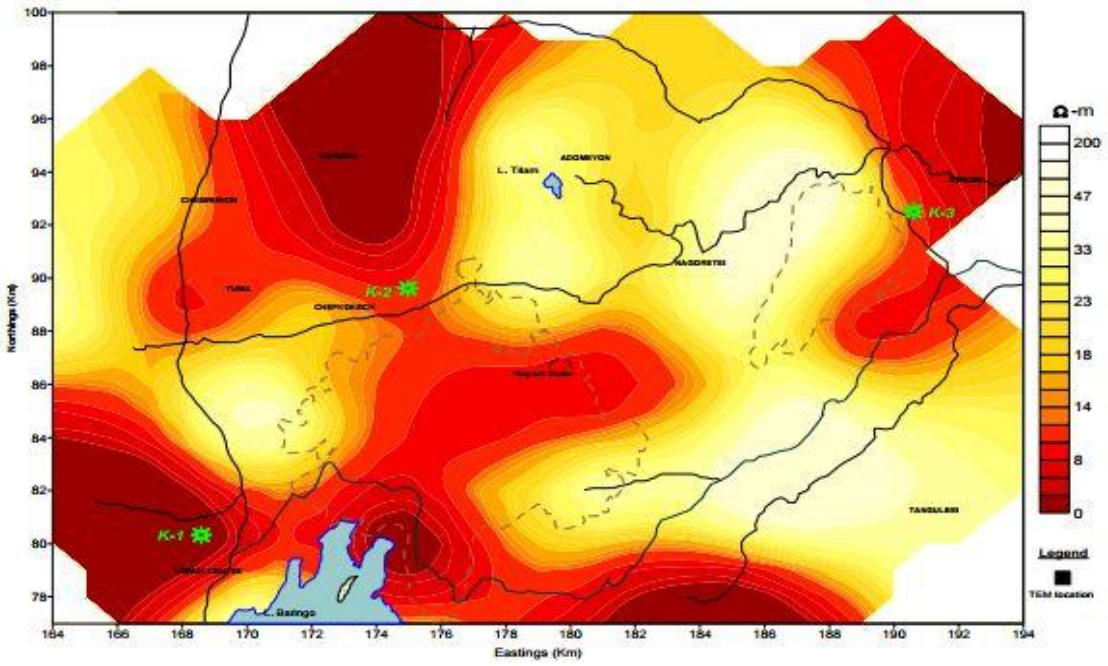

Figure 4.35: Location of the three proposed exploratory wells at Korosi - - Chepchuk prospect superimposed on a TEM resistivity distribution at 450-masl map (JICA, 2010)

4.5.6 Conceptual model

Seismic studies done at the Kenyan North Rift in the early 1990s indicate that the crust thins north of Lake Baringo area and is estimated to be 20-25km thick. Observations from both geological and geophysical studies indicate that dense bodies exist under Korosi volcano as shown in the Figure 4.36. The bodies are expected to provide heat for the geothermal system under Korosi. Intrusions of magma along the NNE structures have also resulted in an emplacement of additional shallow heat sources. It is postulated that the geothermal system at Korosi is still active and that a reservoir exists under the massif with a bias towards the north. Sources of hydrothermal fluids in the Korosi geothermal system are the groundwater from the eastern rift flanks and the Tugen Hills. The high hydraulic gradient between the high recharge areas and the floor allows for deep recharge into the geothermal reservoirs. The fluid flow is enhanced by the highly fractured Plio-Pleistocene lavas that are dominant in this part of the rift. The reservoir rocks are postulated to be Plio-Pleistocene lavas and the associated pyroclastics. The cap rocks are envisaged to be the widespread Korosi tuffs and pyroclastics at depth, which are expected to provide for proper sealing.

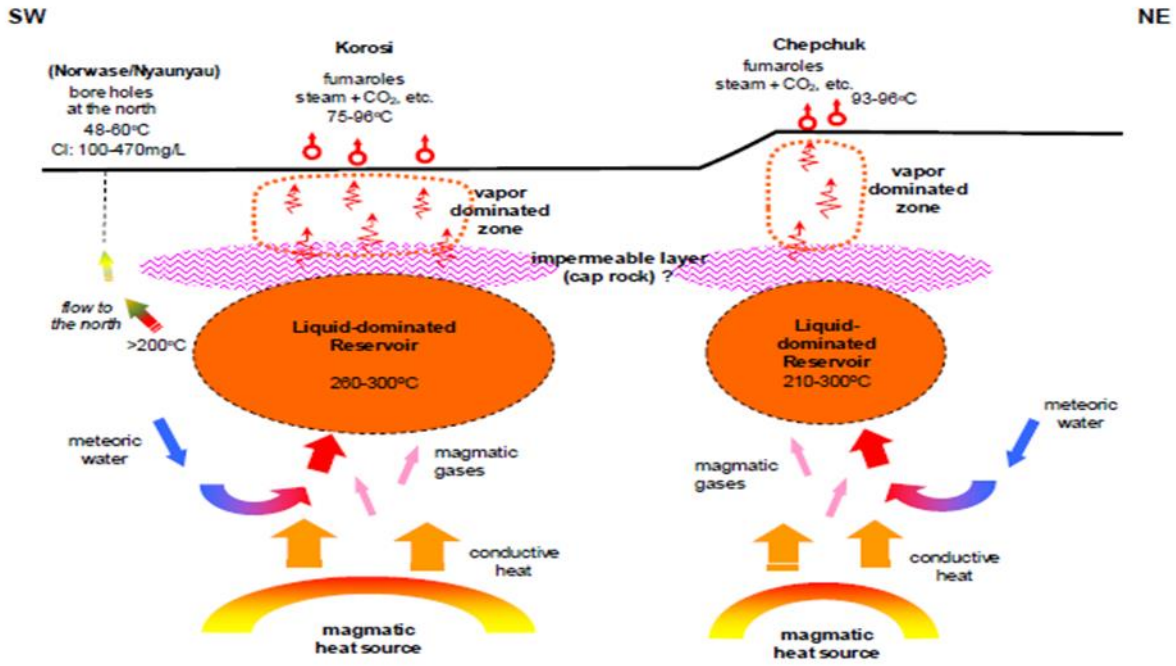

Figure 4.36: simplified geothermal model of Korosi geothermal field (JICA, 2010)

4.5.7 Power potential calculations

Average Temperature = 240 °c

Reservoir area – 25 km² - 45 km²

Power density = 0.0528×250 (°c) ＋1.7917＝ **14.4637**

Power potential range = 14.4637 × 25 km² = **360 MW**

14.4637 × 45 km² = **650 MW**

4.6 SILALI

Silali Volcano is located in the northern Kenyan rift valley, and is bound by the coordinates **1°10'N, 36°12°E.**

4.6.1 Geology

Silali is the largest Quaternary caldera volcano in the northern Gregory Rift and is composed predominantly of peralkaline trachytic lavas and pyroclastic deposits, and mildly alkaline to transitional basalts. It contains a spectacular 8 x 5 km diameter summit caldera, which formed 63,000 years ago. The steep caldera walls are up to 300 m high. The summit of Silali volcano rises 800 m above the surrounding terrain. The floor of the surrounding plain slopes northward from an altitude of 800 m to 600 m towards Emuruangogolak.

The surface features in Silali are manifested to the western slopes of the volcano in form of hot springs at Kapedo while the eastern part is characterized by numerous fumaroles and widespread hot and altered grounds with surface temperatures ranging from 65-90^0 C. The series of springs (Kapedo) to the western side discharge at temperatures of 45-55ºC with a combined estimated flow-rate of about 1,000 l/s.

4.6.2 Volcanology

Detailed mapping combined with radiometric 40Ar/39Ar age determinations is used to constrain the evolutionary development of Silali. Activity commenced at c. 400–220 ka with the construction of a low relief lava shield whose summit area was subsequently modified by alternating periods of faulting, subsidence and infilling associated with two major periods of explosive activity. This activity ceased around 133–131 ka and was probably the result of fracturing and decompression of a high-level magma chamber by regional extension and the injection of basaltic dykes below

the volcano. Later eruptions (c. 120 ka) along the western flanks migrated eastward with time and culminated in the eruption of viscous trachyte lavas from a circumferential fissure zone. The emplacement of a basic dyke swarm to shallow crustal levels beneath Silali resulted in the formation a broad volcanic rift zone within which large volumes of fluid basalts were erupted to mantle the flanks of the volcano. This activity mainly pre-dated, but probably also overlapped with, incremental subsidence and asymmetric down sagging of the summit area.

4.6.3 Geological structure

Early eruptions of Silali volcano formed a 500 m high lava shield. Construction of the shield was followed by eruption of Kapedo tuffs from pyroclastic cones on the western flanks. Eruption of Kapedo tuffs was followed by major eruption of summit trachytes which cover most of the western slopes. Lava was erupted from a fault, rather than from a cone. Eruption of Katenmening basalts from fissures covered all of the western slopes. This stage was followed by development of three cones at the base of the east facing summit scarp. Lava flows from the cones extended northwards. The final stages of Silali volcano evolution involved the emplacement of Black Hills mounds on the upper eastern flanks of the mountain. Geothermal activity is present in the caldera and upper eastern flanks. Some eruptions may have occurred a few hundred years ago. Figure 4.37 represents the faults and the directions of the faults on the silali volcano.

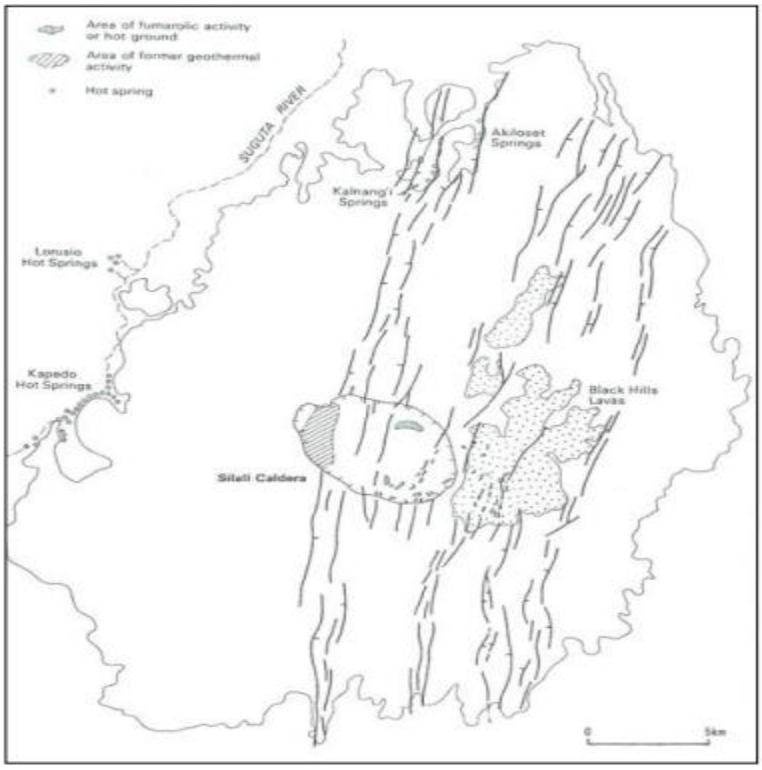

Figure 4.37: Summary of geothermal activity on Silali volcano (Dunkley et al, 1993).

4.6.4 Geochemistry

Geothermometry temperatures from the reconnaissance survey carried out by Dunkley et al., 1992. Silali has some of the largest hot springs within the Kenya rift, indicating high likelihood of existence of a geothermal system under the volcano. It is estimated that Kapedo, which is one of the hot springs, associated with Silali, discharges 1000 liters per second of water at 50 to 55 ℃. This translates into about 100 MW from this region alone. Fluid chemistry, however, indicates that the fluids are not directly from the up flow but have undergone interaction with shallow ground waters. In an area with few surface expressions, carbon dioxide in the soil gas is useful in the search for buried fumarolic activity, determination of geological structures indicating permeability or to confirm presence of potential geothermal areas where other evidence is lacking. The porosity of the formation and other biogenic sources also determine the concentration of carbon dioxide

measured in the soil gas. High carbon dioxide concentration in the soil gas, was observed around hot/altered grounds and fumaroles in Silali prospect as shown in the Figure 4.38. It was found in the north eastern and south eastern areas in and outside the caldera and the eastern parts outside the caldera.

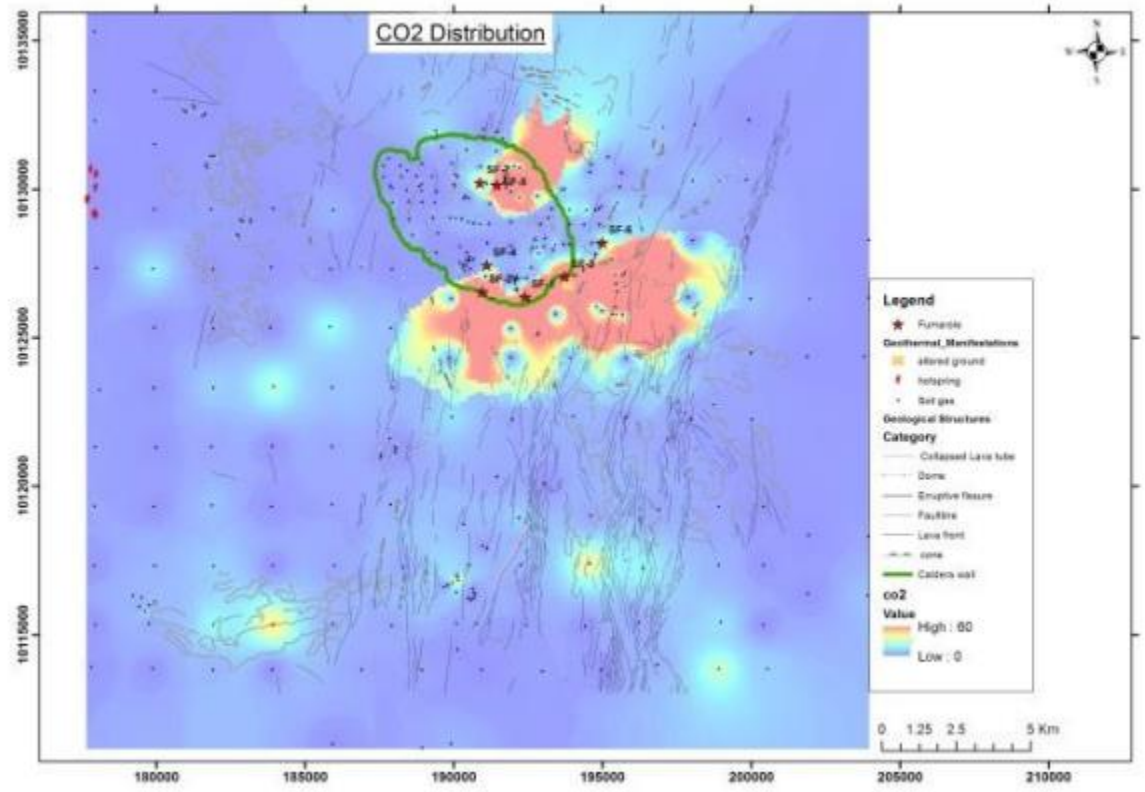

Figure 4.38: Silali prospect CO2 distribution (Dunkley et al, 1993).

4.6.5 Geophysics

4.6.5.1 Gravity

The presence of a positive magnetic anomaly that is coincident with the dimensions of the caldera is further proof of the presence of a hot body under the caldera. High 3He/4He suggests the proximity of the fumaroles in Silali to a shallow magmatic body. Seismic studies indicate high

activity in the east and south east of the caldera floor, which could be related to a geothermal system.

4.6.6 Conceptual model

The model for the system can be explained in terms of an up flow within the caldera with a resource area being probably more than 75 km². The fluid then outflows mainly to the west and north through formational contacts and faults and fractures discharging on the surface at Kapedo springs and other manifestations in the area.

4.6.7 Power potential calculations

Average Temperature = 225 °c

Reservoir area – 30 km² - 75 km²

Power density = 0.0528×225 (°c) ＋1.7917＝ **13.6717**

Power potential range = 13.6717 × 30 km² = **410 MW**

13.6717 × 75 km² = **1025 MW**

4.7 EMURUANGOGOLAK

Emuruangogolak volcano is located 100 km south of Lake Turkana, at the narrowest part of the Baringo-Suguta trough. The rift valley at this latitude is about 125 km, wide.

4.7.1 Geology

The broad Emuruangogolak shield volcano is situated at a narrow constriction in the Gregory Rift and almost completely straddles it. A 5 x 3.5 km summit caldera formed about 38,000 years ago. Since then, trachytic and basaltic lava flows were erupted on the northern and southern flanks and

within the caldera. An NNE-SSW-trending chain of lake-filled basaltic maars extends along the floor of the rift from the lower flanks of the volcano. Young lava flows were also erupted from vents along rift valley faults. Well-preserved parasitic cones erupted along rift-parallel faults cutting the volcano abound; the latest eruption produced a trachytic lava flow dated from secular magnetic variation measurements at about the beginning of the 20th century. Fumarolic activity and hot steaming ground occurs along NNE-trending fissures within the caldera and along the lower NW flanks.

4.7.2 Volcanology

Volcanic activity commenced about one million years ago. Hot ground and fumaroles are located along fissures within the caldera and lower NW flanks. Emuruangogolak has experienced two episodes of summit collapse which produced shallow nested calderas. Parasitic pyroclastic cones situated on the upper western flanks of Emuruangogolak and represent Pre-caldera I Pyroclastic Activity. The dimensions of the first caldera measure 9 × 7.5 km, slightly elongated along a north-west/southeast orientation. The caldera I wall is preserved as a 5 km section running south from Enambaba cone. On the eastern side of the volcano, the caldera I fault is difficult to identify. To the north caldera I rim is buried beneath eruption products from Enambaba and Nakot. The second caldera measures 3.5 × 4.5 km and like the first, is elongated along a north-west/southeast direction. The maximum height of the caldera II wall of 75 m occurs on the south side. Basalt lava was erupted from the summit area soon after the second caldera collapse. The most recent lava flow on Emuruangogolak is a trachyte block lava, erupted from a small cone.

4.7.3 Geochemistry

Geothermal manifestations, some of which are at boiling point, suggests the presence of a geothermal system which gas Geothermometry indicates to be at temperatures of 200℃ to 350 ℃.

Abundance of fumaroles at higher temperatures on the eastern half of the caldera floor may imply a better geothermal system in that segment.

4.7.4 Conceptual model

It is anticipated that the recharge of the geothermal system is good as shown by the occurrence of hot Springs on the eastern flanks of the volcano. It can be modeled that the geothermal fluid up flows within the caldera floor and immediate environs and largely outflows to the north and west.

4.7.5 Power potential calculations

Average Temperature = 200 °c

Reservoir area – 50 km^2 - 70 km^2

Power density = 0.0528×200 (°c) ＋1.7917＝ 12.3517

Power potential range = 12.3517 × 50 km^2 = **615 MW**

12.3517 × 70 km^2 = **865 MW**

4.8 NAMARUNU

Namarunu is located south of the Barrier Volcano in northern Kenya. Hot springs are located at the volcano.

4.8.1 Geology

Namarunu is composed predominantly of Pliocene volcanic sequence which may be broadly correlated with the succession of the rift margin. Quaternary volcanic rocks with pristine Morphological features are superimposed on this older volcanic pile. The succession of Namarunu is described by the Figure 4.39.

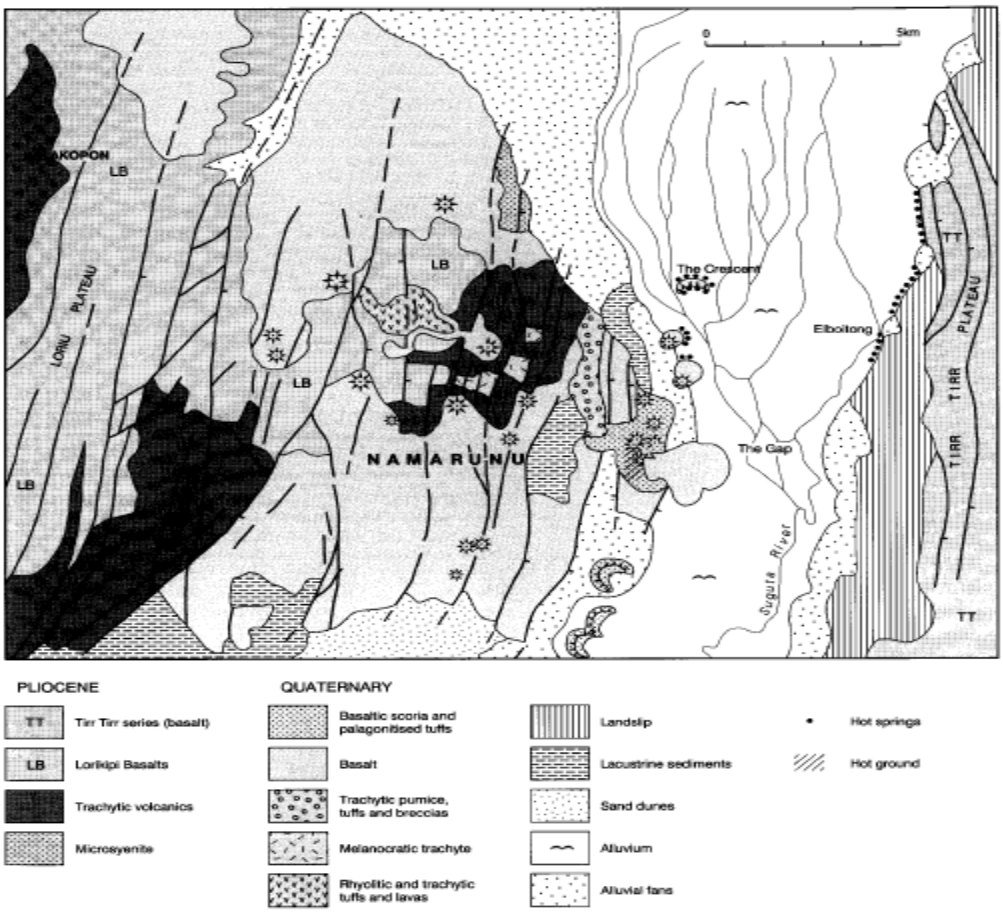

Figure 4.39: Simplified geological map of the Namarunu and adjacent Grounds showing the location of surface Geothermal activity (Dunkley et al, 1993)

4.8.2 Volcanic activity

The largely Pliocene Namarunu trachytic shield volcano is topped by parasitic cones and lava flows of upper Pleistocene and Holocene age. Voluminous basaltic effusive and explosive activity took place during the early Holocene on the lower northern, eastern, and southern flanks along the axis of the East African Rift, producing fissure-controlled subaerial basaltic scoria cones and lava flows, and partially or completely subcrustal tuff cones, tuff rings, and pillow lavas. Fluid olivine basalts were also erupted from a breached scoria cone forming the summit of Namarunu. The youngest eruptions postdated the drying out of Lake Sugata about 3000 years ago. Some could be as recent as the historical eruptions at The Barrier volcano to the north (Dunkley et al., 1993). Hot

springs are located on some of the young volcanic cones on the rift valley floor and on the eastern side of the rift along the base of the Tirr Tirr Plateau.

4.8.3 Geochemistry

Fumaroles at temperatures ranging from 30 to 100 ℃occur at the foot of eastern and western fault scarps. Fluid Geothermometry indicates a reservoir at temperatures of more than 200 ℃. The hottest springs occur along the eastern fault. Hydrological flow patterns indicate that recharge for the Namarunu prospect is largely from the east and south. The hot springs on the west are probably directly associated with a geothermal system in the south and south-east of Namarunu volcanic area. The area is capable of generating more than 20 MW using binary technology.

4.8.4 Conceptual model

Surface geothermal activity within the area is restricted to two zones. By far the most important manifestations are the Elboitong hot springs, which were situated on the eastern side of the Suguta valley at the base of the Tirr -Tirr escapnment. The other zone of activity is associated

4.8.5 Power potential calculations

Average Temperature = 190 °c

Reservoir area – 30 km² - 45 km²

Power density = 0.0528×190 (°c) ＋1.7917＝ **11.8237**

Power potential range = 11.8237 × 30 km² = **355 MW**

= 11.8237 × 45 km² = **540 MW**

4.9 BARRIER GEOTHERMAL FIELD

The Barrier volcanic complex separates Lake Turkana from the broad Suguta Trough to the south, the site of a former lake.

4.9.1 Geology

The volcano is comprised of four overlapping shield volcanoes, with the youngest, Kakorinya, located over the axis of the East African Rift. Kalolenyang volcano lies west of Kakorinya, and Likaiu West and Likaiu East volcano are located to the ENE. A 3.8-km-wide summit caldera was formed at Kakorinya volcano about 92,000 years ago. Youthful-looking trachytic and Phonolitic lava domes and flows erupted within the caldera and along its ring fracture fill much of the caldera floor. Early Holocene fissure-related scoria cones and lava flows dot the volcano's southern and northern flanks. Solfataric fields are located within the caldera and on the western and southern flanks of the volcano. Historical eruptions from Teleki's and Andrew's cones on the northern and southern flanks, respectively, have produced basaltic explosive activity and lava flows during the 19th and 20th centuries.

4.9.2 Volcanology

The complex consists of three volcanoes of which Kakorinya is the most promising in terms of geothermal potential. Kakorinya is a silicic volcanic center whose caldera formation was accompanied by a collapse about 92,000 years ago, followed by resurgence activity about 58,000 years ago. A caldera association implies that the volcano developed shallow magma chamber whose heat could still drive a geothermal system. Recent basaltic activity at Teleki's volcano (100 years) is a strong indicator that new magma injections still occur, which could raise the local geothermal potential.

4.9.3 Geochemistry

Developing a geothermal model for the prospect is complicated by lack of geophysical data and conflicting geochemical information. Low H2 and CH4 in the fumaroles and springs indicate an indirect path between the discharges and the heat source suggesting that the potential for the area is low. In contrast, high gas Geothermometry temperatures (218 to 328 ℃) suggest proximity to an up flow.

4.9.4 Conceptual model

It is likely that a high temperature geothermal system exists under the Kakorinya volcano with temperature in excess of 300°C. Sulphur deposits that are indicative of shallow, degassing magmas occur within the caldera, further indicating that a large heat source exists under the volcano. Fracture-controlled permeability is defined by NNE-trending faults dominating the up-flow and outflow in the system. The reservoir rocks at a depth of between 2,000m and 3,000m are inferred to be fractured and highly altered trachytes whereas recharge into the geothermal system is provided by master rift faults with minor components from the axial rift flow. Preliminary indications are that the resource is capable of generating more than 100 MW.

4.9.5 Power potential calculation

Average Temperature – 250 °c

Reservoir area – 20 km² - 50 km²

Power density = 0.0528×250 (°c) ＋1.7917＝ **14.9917**

Power potential range = 14.9917 × 20 km² = **300 MW**

= 14.9917 × 50 km² = **750 MW**

5 CONCLUSIONS AND RECOMMENDATIONS

5.1 CONCLUSIONS

Taking the resource capacity estimates, geological, hydrogeological, and fluid chemistry criteria into consideration and some socio-economic factors, the geothermal prospects are ranked as follows:

A. Suswa, Longonot and Silali are high temperature geothermal fields associated with young trachytic magmatic events and should be given priority in development. These geothermal fields are categorized into class A.

B. Emuruangogolak, Korosi and Barrier geothermal field can be characterized second in terms of ranking because they are moderately hot geothermal system and are worthy of further exploration. There is little to choose between the three from a purely geological point of view and can be given equal opportunity in terms of development. These geothermal fields have been characterized into class B.

C. Arus Bogoria and Lake Baringo can be characterized third because of the influence of heat losses and their proximity to the lake. They are however intermediate to hot geothermal fields. Arus Bogoria and Lake Baringo are graded as class C in terms of ranking because of their heat losses.

D. Namarunu is ranked last because of it's a Pleistocene volcano and there are extremely weak geothermal manifestations. It is thus considered poor geothermal field however it can still merit for geothermal development. Namarunu is ranked in class D due to their weak geothermal manifestation.

1. Suswa
2. Longonot

3. Silali
4. Emuruangogolak
5. Korosi
6. Barrier
7. Arus Bogoria
8. Lake Baringo
9. Namarunu

As discussed above class A geothermal fields show strong geothermal characteristics and higher energy capacities, class B shows better geothermal characteristics but not as good as A. finally we have class C and class D geothermal fields which show weak geothermal characteristics. These classes show their rank to development in reference to resource capacity estimates, geological, hydrogeological and volcanological data.

Table 1: Classification and ranking of the various geothermal fields

	Geothermal field	**Resource potential**	**Ranking**
1	Suswa	410 Mw - 680 Mw	A
2	Longonot	520 Mw -750 Mw	A
3	Silali	410 Mw -1025 Mw	A
4	Emuruangogolak	615 Mw -865 Mw	B
5	Korosi	360 Mw -650 Mw	B
6	Barrier	300 Mw -750 Mw	B
7	Arus Bogoria	247 Mw - 430 Mw	C
8	Lake Baringo	247 Mw -308 Mw	C
9	Namarunu	255 Mw -540 Mw	D

5.2 RECOMMENDATIONS

I. It is recommended that further exploration to be done on these volcanoes to delineate the best drilling sites

II. It is also recommended a detailed hydrogeological surveys to determine the water tables, temperature change and rock permeability in each field.

6 REFERENCES

Achauer, U., and Masson, F., (2002): Seismic tomography of continental rifts revisited: from relative to absolute heterogeneities. Tectonophysics, 358, 17-37.

Allen, D. M., Ghomshei, M. M., Sadler-Brown, T. L., Dakin, A., & Holtz, D. (2000, May). The current status of geothermal exploration and development in Canada. In Proceedings from World Geothermal Congress (pp. 55-58).

Alexander, K. B., Ussher, G., & Merz, S. K. (2011, October). Geothermal resource assessment for Mt Longonot, Central Rift Valley, Kenya. In Proceedings of the GRC Annual Meeting, San Diego, CA, USA (pp. 23-26).

Árnason, K., & Gíslason, G. (2009). Geothermal surface exploration. Makalah disajikan dalam Short Course on Surface Exploration for Geothermal Resources, United Nations University Geothermal Training Programme and LaGeo, El Salvador, 17-30.

Axelsson, G., Arnaldsson, A., Gylfadóttir, S. S., Halldórsdóttir, S., Mortensen, A. K., Bore, C., Karingithi, C., Koech, V., Mbithi, U., Muchemi, G., Mwarania, F., Opondo, K., & Ouma, P. (2013). Conceptual model and resource assessment for the Olkaria geothermal system, Kenya.

Baker, B.H., Mohr, P.A., and Williams, L. A. J., (1972): Geology of the Eastern Rift System of Africa. Contrib. GSA Special Papers, 136, 1-68.

Baker, B.H. and Wohlenberg, J., (1971): Structural evolution of the Kenya Rift Valley. Nature, 229, 538 542.

Bauer, M., Freeden, W., Jacobi, H., & Neu, T. (2014). Handbook of deep geothermal energy. Springer Berlin Heidelberg.

Boone, S. C., Kohn, B. P., Gleadow, A. J., Morley, C. K., Seiler, C., & Foster, D. A. (2019). Birth of the East African Rift System: Nucleation of magmatism and strain in the Turkana Depression. Geology, 47(9), 886-890.

Brown, D. W., Duchane, D. V., Heiken, G., & Hriscu, V. T. (2012). Mining the earth's heat: hot dry rock geothermal energy. Springer Science & Business Media.

Calais, E., Ebinger, C., Hartnady, C., & Nocquet, J.-M. (2006). Kinematics of the East African Rift from GPS and earthquake slip vector data. Geological Society, London, Special Publications, 259, 9–22. https://doi.org/10.1144/GSL.SP.2006.259.01.03

Chorowicz, J., (2005): The East African Rift System. J. African Earth Sciences, 43, 379-410.

Debout, D. G., Weise, B. R., Gregory, A. R., & Edwards, M. B. (1982). Wilcox sandstone reservoirs in the deep subsurface along the Texas Gulf Coast: their potential for production of geopressured geothermal energy. Report of Investigations No. 117 (No. DOE/ET/28461-T2). Texas Univ., Austin (USA). Bureau of Economic Geology.

Dunkley, P.N., Smith, M., Allen, D.A. and Darling, W.G, (1993). The geothermal activity and geology of the northern sector of the Kenya Rift Valley. British Geological Survey Research Report, SC/93/1.

Ebinger, C., (2005): Continental breakup: The East African perspective. Astronomy and Geophysics, 46, 216–221.

Ebinger, C., and Sleep, N.H., (1998): Cenozoic magmatism in central and east Africa resulting from impact of one large plume. Nature, 395, 788–791.

Gehringer, M., & Loksha, V. (2012). Geothermal Handbook.

Geotermica Italiana Srl (1987). Geothermal Reconnaissance Survey in the Menengai-Bogoria Area of the Kenya Rift Valley. Final Report.

Hamilton, R. M., & Muffler, L. J. P. (1972). Microearthquakes at the Geysers geothermal area, California. Journal of Geophysical Research, 77(11), 2081-2086.

Hay, D. E., & Wendlandt, R. F. (1995). The origin of Kenya rift plateau- type flood phonolites: Results of high- pressure/high- temperature experiments in the systems phonolite- H2O and phonolite-H2O- CO2. Journal of Geophysical Research: Solid Earth, 100(B1), 401-410.

Hervey, C., Beardsmore, G., Moeck, I., Ruter, H., & Bauer, S. (2014). Best practices guide for geothermal exploration.

House, P. A., Johnson, P. M., & Towse, D. F. (1975). Potential power generation and gas production from Gulf Coast geopressure reservoirs (No. UCRL-51813). California Univ., Livermore (USA). Lawrence Livermore Lab.

JICA, 2010: Technical report on geothermal exploration in Eburru field rift valley- republic of Kenya, JICA geothermal mission.

Kanoglu, M. (2002). Exergy analysis of a dual-level binary geothermal power plant. Geothermics, 31(6), 709-724.

Karingithi C.W., 2005: Geochemical report of Arus and Bogoria geothermal prospects, Kenya

Electricity Generating Company, Ltd, internal report, 24 pp.

Karingithi, C. W. (2009). Chemical geothermometers for geothermal exploration. In Short Course IV on Exploration for Geothermal Resources (Vol. 1). Lake Vaivasha, Kenya: United Nations University, Geothermal Training Program.

KenGen, 1998. Surface scientific investigation of Longonot geothermal prospect. Kenya Electricity Generating Company Ltd., internal report, 91 pp.

KenGen, (1999). Suswa and Longonot geothermal prospects. Comparison of surface scientific data.

KenGen, internal report, 30 pp. KenGen, (2004) Lake Baringo Geothermal Prospect report

Kenya Geological Survey, (1960) Menengai-Bogoria reconnaissance report.

Lagat, J., 2003. Geology and the geothermal systems of the southern segment of the Kenya Rift. #S04, Paper 107, International Geothermal Conference, Reykjavik, September 2003.

Lagat, J. (2008, November). Geology and geothermal resource utilization options in the Arus-Lake Bogoria prospect, northern Kenya rift. In Proceedings ARGeo 2 Conference, Entebbe, Uganda, 24-26 November 2008.

Mariita, N. O. (2003). An integrated geophysical study of the northern Kenya rift crustal structure: implications for geothermal energy prospecting for Menengai area. The University of Texas at El Paso.ka

Marshall, A.S., Macdonald, R., Rogers, N.W., Fitton, J.G., Tindle, A.G., Nejbert, K., and Hinton, R.W., (2009): Fractionation of peralkaline silicic magmas: The Greater Olkaria volcanic complex, Kenya Rift -Valley. J. Petrology, 50, 323-359.

Ministry of Energy (1986) Geothermal exploration unpublished report.

Omenda .P.A., Opondo K., Lagat J., Mungania J., Mariita N., Onacha S., Simiyu S., Wetang'ula G., Ouma P., 2000: Ranking of geothermal prospects in the Kenya rift. Kenya Electricity Generating Company Limited, internal report. pp 121.

Omenda, P. A., & Karintithi, C. W. (1993). Hydrothermal model of Eburru geothermal field, Kenya. In The 1993 Annual Meeting on Utilities and Geothermal: An Emerging Partnership, Burlingame, CA, USA, 10/10-13/93 (pp. 155-160).

Omenda, Peter, Peketsa Mangi, Cornel Ofwona, and Martin Mwangi. "Country update report for Kenya 2015-2019." In Proceedings of World Geothermal Congress. 2020.

Omenda, P., & Simiyu, S. (2015). Country update Report for Kenya: 2010-2014. World Geothermal Congress (p. 11). Melbourne: International Geothermal Association.

Onacha, S. A. (2006). Hydrothermal fault zone mapping using seismic and electrical measurements.

Parri, R., & Lazzeri, F. (2016). Larderello: 100 years of geothermal power plant evolution in Italy. In Geothermal Power Generation (pp. 537-590). Woodhead Publishing.

Riaroh, D., & Okoth, W. (1994). The geothermal fields of the Kenya rift. Tectonophysics, 236(1-4), 117-130.

Ring, U., (2014): The East African Rift System: Austrian J. Earth Sciences, 107-1, 132-146.

Rybach, L., & Muffler, L. J. P. (1981). Geothermal systems: principles and case histories. Chichester.

Saemundsson, K., Axelsson, G., & Steingrímsson, B. (2009). Geothermal systems in global perspective. Short course on exploration for geothermal resources, UNU GTP, 11.

Shackleton, R.M., (1996): The final collision between East and West Gondwana: where is it? J. African Earth Sciences, 23, 271-287.

Simiyu, S. M. (2010, April). Status of geothermal exploration in Kenya and future plans for its development. In Proceedings world geothermal congress (pp. 25-29).

Smith, M., Mosley, P., (1993): Crustal heterogeneity and basement influence on the development of the Kenya Rift, East Africa. Tectonics 12-2, 591–606.

Tester, J., Blackwell, D., Petty, S., Richards, M., Moore, M., Anderson, B., ... & Garnish, J. (2007, January). The future of geothermal energy: an assessment of the energy supply potential of engineered geothermal systems (EGS) for the United States. In Proc. of the Thirty-Second Workshop on Geothermal Reservoir Engineering, Stanford University, Stanford, California, USA.

Tongue, J., Maguire, P., & Burton, P. (1994). An earthquake study in the Lake Baringo basin of the central Kenya Rift. Tectonophysics, 236(1-4), 151-164.

Williams, L.A.J., (1970): The volcanics of the Gregory Rift Valley, East Africa. Bull. Volcanology, 34, 439-465.

Wilmarth, M., & Stimac, J. (2014, February). Worldwide power density review. In Proceedings, Thirty-Ninth Workshop on Geothermal Reservoir Engineering, Stanford University, Stanford, CA, USA (pp. 24-26).

Wilson, M. (Ed.). (1989). Igneous petrogenesis. Dordrecht: Springer Netherlands.